DEVELOPMENT OF NITRILE BUTADIENE RUBBER (NBR)/GRAPHENE OXIDE (GO) MEMBRANE FOR OILY WASTEWATER FILTRATION – CURING OPTIMIZATION STUDY

NAGARATHANAM A/P RAMADAS

A project report submitted in partial fulfilment of the requirements for the award of the degree of Bachelor of Engineering (Hons) Petrochemical Engineering

Faculty of Engineering and Green Technology
Universiti Tunku Abdul Rahman

April 2018

DECLARATION

I hereby declare that this project report is based on my original work except for citations and quotations which have been duly acknowledged. I also declare that it has not been previously and concurrently submitted for any other degree or award at UTAR or other institutions.

Signature : _____

Name : Nagarathanam a/p Ramadas

ID No. : 13AGB06663

Date : _____

APPROVAL FOR SUBMISSION

I certify that this project report entitled **"DEVELOPMENT OF NITRILE BUTADIENE RUBBER (NBR)/GRAPHENE OXIDE (GO) MEMBRANE FOR OILY WASTEWATER FILTRATION – CURING OPTIMIZATION STUDY"** was prepared by **NAGARATHANAM A/P RAMADAS** has met the required standard for submission in partial fulfilment of the requirements for the award of Bachelor of Engineering (Hons) Petrochemical Engineering at Universiti Tunku Abdul Rahman.

Approved by,

Signature : _____

Supervisor : Dr. Yamuna a/p Munusamy

Date : _____

Specially Dedicated to

Faculty of Engineering and Green Technology (FEGT), Petrochemical Engineering (PE) Department, All the Lecturers, My Beloved Mother, Family and Friends

ACKNOWLEDGEMENTS

"Dear GOD, Thank You for giving me the strength and courage throughout the journey in completing this thesis. I am truly grateful to be under Your blessings."

I would like to express my deepest appreciation to all those who provided me the possibility to complete this project. A special gratitude I give to my research supervisor, Dr. Yamuna a/p Munusamy for her invaluable advice, guidance and her enormous patience throughout the development of the research.

I would also like to thank my moderator Dr. Lai Koon Chun, the lecturers and lab officers of UTAR especially Dr. Mathialagan a/l Muniyadi who had given me a lot of assistance and advice during the course of the project.

In addition, I would like to express my gratitude to my loving mother Mdm. Rajaesperi, my family and friends for their endless love and encouragement. Their continuous support and guidance are the backbone for the successful completion of this project. Lastly, I would like to express my appreciation to everyone who had supported me along the way for the successful completion of this project.

DEVELOPMENT OF NITRILE BUTADIENE RUBBER (NBR)/GRAPHENE OXIDE (GO) MEMBRANE FOR OILY WASTEWATER FILTRATION – CURING OPTIMIZATION STUDY

ABSTRACT

Membrane technology is one of the promising method that could be developed to remove emulsified oil in wastewater. In this study, Nitrile Butadiene Rubber (NBR)/Graphene Oxide (GO) membranes which are suitable for oily wastewater filtration were developed through latex compounding and curing method. Graphite oxide was synthesized from graphite nanofibre (GNF) using conventional Hummer's method. Fourier Transform Infrared Spectroscopy (FTIR) proved the successful oxidation of GNF to graphite oxide. Graphite oxide was infused into NBR to produce NBR/GO nanocomposite membranes at loadings of 0.5, 1.0, 1.5 and 2.0 wt% through latex compounding method to determine the optimum loading of GO for NBR/GO membrane. The curing temperature was fixed at 100 °C and two different curing times which were 2 and 3 hours were set to find out the optimum curing time for NBR and NBR/GO membranes. The NBR and NBR/GO membranes were characterized by Fourier Transform Infrared Spectroscopy (FTIR), Field Emission Scanning Electron Microscopy (FESEM) and X-Ray Diffraction (XRD). FTIR evidenced hydrogen bond formation between GO and NBR. XRD proved that interlayer spacing affected by the intercalation of graphite oxide sheets in NBR. GO and pores could be observed at the surface of the NBR latex membrane through FESEM images. Mechanical properties of the NBR and NBR/GO membranes were investigated by tensile test. Results showed that the Young's Modulus, tensile strength and elongation at break of NBR/GO membranes cured for 2 hours showed increment when compared with pure NBR membrane. The performance of NBR and NBR/GO membranes were analyzed in terms of permeation flux and oil rejection rate. NBR and NBR/GO membranes were tested at pressure of 0.5 bar to investigate the flux behavior using synthetic oily

wastewater. Based on the results obtained, pure NBR membrane was unable to filter the oily wastewater and only the NBR/2.0 wt% GO membrane cured for 2 hours was able to filter the oily wastewater. The permeation flux obtained was $544.11\left(\frac{L}{m^2.hr}\right)$. The result from permeation flux was further facilitated with the oil rejection rate test based on COD and TOC. The oil rejection rate based on TOC obtained is 85.5 % while the oil rejection rate based on COD is 58.6 %. The results and data retrieved showed that NBR/GO membrane could reject oil. It can be concluded that the optimum curing time and GO formulation for NBR and NBR/GO membranes are 2 hours and 2.0 wt% respectively.

Keywords: Graphene Oxide; Nitrile Butadiene Rubber; Nanocomposite Membrane; Loading of GO; Curing Time

TABLE OF CONTENTS

LIST OF TABLES

LIST OF FIGURES

LIST OF SYMBOLS / ABBREVIATIONS

ACN	acrylonitrile
BOD	biological oxygen demand
CNTs	carbon nanotubes
COD	chemical oxygen demand
DAF	dissolved air flotation
FESEM	Field Emission Scanning Electron Microscopy
FTIR	Fourier Transform Infrared Spectroscopy
GNP	graphene nanoplateles
GO	graphene oxide
HRTEM	high-resolution transmission electron microscopy
IBAFs	immobilized biological aerated filters
MF	microfiltration
NBR	nitrile butadiene rubber
NF	nanofiltration
NMR	Nuclear Magnetic Resonance
PAN	polyacrylonitrile
PSF	polysulfone
PSNTs	phosphorylated silica nanotubes
PTFE	polytetrafluoroethylene
PVDF	polyvinylidenedifluoride
RO	reverse osmosis
SS	suspended solid
TOC	total oil content
TSC	total solid content
UASB	up flow anaerobic sludge blanket
UF	ultrafiltration

XRD	X-Ray Diffraction
λ	wavelength
d	interlayer spacing (Armstrong)
J_p	Permeate Flux, $\frac{L}{m^2.hr}$
V_p	Permeate volume collected, *L*
A	Effective membrane area, m^2
t	Time taken to collect the measured amount of permeate, *hr*
R	Rejection rate, %
C_p	Concentration in the permeate, mg/L
C_f	Concentration in the feed, mg/L

LIST OF APPENDICES

CHAPTER 1

INTRODUCTION

1.1 Background

Rapid industrial development in oil and gas, petrochemical, pharmaceutical, metallurgical and food sector, has contributed to the large production of oily wastewater (Padaki et al., 2014). Oily wastewater is wastewater mixed with oil under a broad range of concentrations. The oil mixed in water, can be fats, hydrocarbons and petroleum fractions like diesel oil, gasoline and kerosene. Nowadays, many industries generate a great quantity of oily wastewater, which cause various adverse impacts on the surrounding environment such as pollution and hydrocarbon contents to the atmosphere (Jamaly, Giwa and Hasan, 2015). Oily wastewater pollution mainly affects drinking water and groundwater resources, endangering aquatic resources and human health, causing atmospheric pollution, affecting crop production and destructing the natural landscape (Yu, Han and He, 2013). So, an inevitable challenge is the necessity to treat the oily wastewater.

Furthermore, the rapid growths in population and economy have resulted in greater demand for clean water, specifically in water-stressed areas (Salahi et al., 2013). Thus, the present surface resources will be no longer adequate to satisfy the demands of future generations (Padaki et al., 2014). Oily wastewater treatment has become of great significance in the latter years. Proper treatment combined with adequate water quality auditing, maintenance and distribution, is vital to grant safe and affordable clean water supply (AlMarzooqi et al., 2014; Macedonio et al., 2012). There are many methods to treat oily wastewater such as gravity separation, skimming, dissolved air

flotation (DAF), flocculation, de-emulsification methods, electro flotation, electro coagulation, chemical emulsion breaking, mechanical coalescence, micro and ultrasonic wave treatment and so on. All these traditional methods have drawbacks such as they are only useful for free oil solutions and dispersed/unstable oil/water emulsions when the concentration of oil is very low. In addition, another four conventional treatment methods of oily wastewater are flotation, coagulation, biological treatment and membrane separation technology (Yu, Han and He, 2013). These conventional systems can be used to readily remove the free and dispersed form of oil.

Oil in oily wastewater can exist in free, dispersed and emulsion form (Asatekin and Mayes, 2009). It is hard to remove the emulsified oil from wastewater. Commonly, in oily wastewater the oil exists in highly stable emulsion form due to certain process and chemical that was added to cause oil to dissolve in water. Therefore, the wastewater needs to be pre-treated physically or chemically to break and remove emulsion prior to filtration (Roads & Bridges, 2017).

According to previous researches membrane technology is one of the promising method that could be developed to remove emulsified oil in wastewater (Maguire-Boyle and Barron, 2011; Fakhru'l-Razi et al., 2009; Ashaghi, Ebrahimi and Czermak, 2007; Padaki et al., 2014). Membranes are preferred because no additional chemical or thermal inputs are required (Pendergast, 2011). The membrane functions as a very specific filter that will allow water permeation through it, while it rejects solids and oil based on the principles of size exclusion and selective permeability (Klaysom et al., 2013).

Figure 1.1 shows the classification of membranes based on pore size. Microfiltration (MF) membrane removes suspended particles, bacteria and some viruses whereas ultrafiltration (UF) membrane removes viruses, proteins and colloidal particles. Nanofiltration (NF) membrane is selective for multivalent ions and dissolved compounds and reverse osmosis (RO) membrane, usually allows only water to pass through. Membranes can be functioned in either dead-end filtration or cross-flow filtration. The retentate concentrates on the membrane in dead-end filtration whereas the permeate leaves through the pores of the membrane, and the concentrated retentate

flows away over the membrane in cross-flow filtration. Flat-sheet or hollow fiber membranes can be used based on the operating conditions of the membrane. Flat-sheet membranes can be rolled into a spiral-wound modules or used in a plate-and-frame setup. Hollow fiber modules contain several hundred to thousands of fibers (Dickhout et al., 2016).

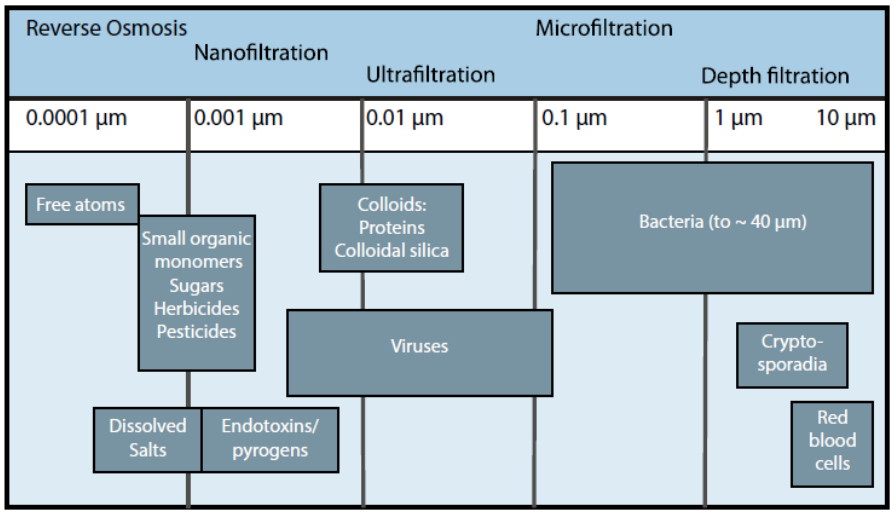

Figure 1.1: Classification of membranes based on pore size (Dickhout et al., 2016).

Dickhout et al. (2016) stated that membranes can be divided into two groups based on the materials they are made of, namely polymeric or ceramic. The membranes that made from materials such as silica, metal oxides or carbon known as ceramic or inorganic membranes. They have superior thermal and chemical stability, and their use in industrial application of oil recovery is an emerging technology.

Polymeric membranes are used in different separation processes in industry. Selecting a polymeric membrane for a certain task is not a trivial exercise, because the polymer has to have the right affinity and has to withstand the environment of the separation. Polymeric membranes can be either produced from pure polymers or from polymers blends to improve the membrane performance (Lalia et al., 2013). Other than that, it also can be made both dense and porous, depending on the application, whereas modifications on the membrane surface can be made to improve the functionality of the membrane (Khulbe, Feng and Matsuura, 2010).

The outstanding features of carbon nanomaterials ever since their disclosure have drawn a huge attention (Ku, Lee and Park, 2012). Nanocomposite membrane based water treatment is expected to play an increasingly crucial role in wastewater treatment and reuse. The idea of utilizing the advantages of nanofillers as a choice for membrane material is expected to develop a superior nanocomposite membrane with enhanced flux, improved rejection rate and other enticing characteristics. The nanocomposite membranes offer favourable permeation for selective transport while acting as a barricade for undesired transport (Mondal, 2015).

Besides that, establishment of novel nanocomposite polymeric membrane by structural alteration of the current matrix of polymer membrane materials in order to improve their permeability, selectivity, strength and other properties would play an important role in membrane science and technology (Mondal, 2015). In the recent years, polymer nanocomposite membrane has been domineering in its application for gas separation, water and wastewater treatment, desalination, and many more. Potential nanofillers for polymer nanocomposite membrane preparation are carbon nanotubes (CNTs), graphene oxide (GO) and clay (Lawler, 2016). By reinforcing nanofillers in the polymer membrane matrix, improvement of membrane permeability and selectivity during filtration could be attained (Ganesh, Isloor and Ismail, 2013; Lee et al., 2013).

1.2 Problem Statement

Conventional oily wastewater treatment methods have their own drawbacks; high cost, using toxic compounds, large space for installation and generation of secondary pollutants. Membrane separation processes serve as an emerging technology in the 21st century, when keeping these drawbacks in view. However the oil components can cause fouling of the membrane easily (Asatekin and Mayes, 2009) leading to lower efficiency of the membrane. In other word, the membrane fouling stays as one of the main technical challenge in the wastewater separation industries (Padaki et al., 2014). This is due to the fact that polymeric membrane has acquire inherent hydrophobic surface which is subjected to fouling and hindering the membrane to perform well

(Sun et al., 2014). Fouling mechanisms can be categorized in five different processes, shown in Figure 1.2 and those processes have possibility to take place at the same time.

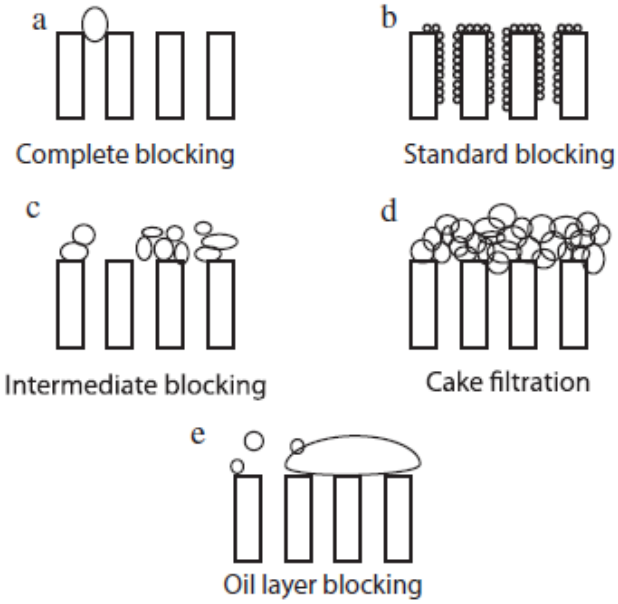

Figure 1.2: Schematic representation of the different fouling mechanisms taking place on the membrane surface (Dickhout et al., 2016).

Besides, another common limitation of the polymeric membrane is the trade-off effect between the permeation flux and rejection rate (Song, 1998; Kong and Li, 1999; Belkacem et al., 1995). Polymeric membrane are poor mechanical strength and chemical resistance (Zavastin, 2010). The key for an ideal membrane is a membrane that does not foul and have no trade-off effect. This will directly aid in saving operating costs, provide higher efficiency, require low energy and produce high purity water (Gryta, Karakulski and Morawski, 2001; Yang et al., 2011). A new access is needed to provide an alternate and cost-effective membrane. This suggests that membranes need hydrophilic alteration of the existing hydrophobic surface. Hence, research and developments are conducted to enhance the properties of the membrane by the addition of nanomaterials (Zhu et al., 2014).

The disadvantages of the conventional methods and membrane technology short comings have brought to the advancement in nanocomposite membranes. Many studies have proven that development of nanocomposite membranes have enhanced

membranes properties such as selectivity, stability and permeability rather than the pure polymeric membrane. Incorporation of various nanoparticles into the polymer membrane layers may modify the network structure of the membranes and directly improves and increases the water flux (Sean, Cheer and Ismail, 2015).

In this study, improvisations are made to produce synthetic latex based nitrile butadiene rubber (NBR)/GO membrane through latex compounding and curing method. NBR has never been used in membrane development. NBR polymer is chosen in this study due to its excellent features such as outstanding chemical and physical properties, and good oil resistance (Paran, Naderi and Ghoreishy, 2016). The NBR matrix if crosslink adequately will exhibit high mechanical properties (Thomas and Stephen, 2010).

GO nanofiller has been chosen in this research due to the fact that previous researches have successfully proven improved performance of membrane properties by the reinforcement of GO in the membrane (Cui, Kundalwal and Kumar, 2016). Besides that, addition of GO into membranes for water treatment is preferred because it increased permeability due to oxidation of the pristine graphene structure (Wilkinson, 2017). GO is an upcoming membrane nanofiller which give promising enhancement on membrane performance in terms of increasing flux, rejection rate, hydrophilicity as well as mechanical strength (Macedonio et al., 2012).

In this study, the curing temperature was fixed at 100 ºC because from our previous study, the optimum water flux and rejection rate was obtained at this temperature. Focus was given more on the GO loading and curing time of the NBR latex matrix. The NBR and NBR/GO membranes were produced using latex compounding and curing method which is different from phase inversion method. Thus, the manipulation of curing properties will influence the performance of NBR and NBR/GO membranes. The performance of the NBR and NBR/GO membranes are tested and compared in terms of permeation flux and oil rejection rate.

1.3 Aims and Objectives

The aim of this study is to produce and optimize the performance of NBR and NBR/GO membranes through latex compounding and curing method. The performance of the membrane in term of water flux and rejection rate will be studied. The mechanical properties of the membrane will be evaluated.

The objectives of the research work are shown as follows:

i) To develop NBR and NBR/GO membranes, which are suitable for oily wastewater filtration through latex compounding and curing method.
ii) To study the curing times and the GO formulations effect on properties of NBR and NBR/GO membranes.
iii) To characterize NBR and NBR/GO membranes and test the tensile properties.
iv) To test the performance of the NBR and NBR/GO membranes in terms of permeation flux and oil rejection rate.

CHAPTER 2

LITERATURE REVIEW

2.1 Oily Wastewater Conventional Treatment Methods

There is no suspicion that the surging extent of industrialization, has led to the large formation of oily wastewater. The necessity to filter oil from oily wastewater is an unavoidable challenge. In addition, the increase in population and the current global water shortage problem have resulted in higher demand for clean water (Salahi et al., 2013). As a whole, these factors have motivate many researchers and scientists toward the advancement in useful techniques and approaches to produce water of a quality that is suitable for usage (Almarzooqi et al., 2014; Macedonio et al., 2012). Conventional techniques in treating oily wastewater include flotation, coagulation, biological treatment and membrane separation technology (Asatekin and Mayes, 2009).

2.1.1 Flotation

Flotation impeller, dissolved air flotation, and jet impeller flotation methods are the conventional flotation treatment for wastewater. Dissolved air flotation (DAF) exploits the presence of air to elevate the buoyancy of smaller oil droplets and enhance the separation process. Oil emulsion is removed by de-emulsification with chemicals, thermal energy or both (Tang and Liu, 2006).

Pre-treatment is usually required for emulsified oil. The intention is to destabilize the emulsion and then it can be separated by gravity separation. Chemical emulsion breaking has several limitations although it is effective. The drawbacks from the chemical emulsion breaking are such as the process is highly vulnerable to changes in influent quality, needs close control and talented operators during operation, needs customization depending on the site to determine the type and quantity of chemicals required and it generates large volumes of sludge. On top of that, depending on the application and the occurrence of corrosion problems caused by the chemicals, the operating costs can be expensive. Emulsion can also be treated physically with methods for breaking emulsions consist of centrifugation, pre-coat filtration, heating, fibre beds, ultrafiltration and reverse osmosis, and electrochemical treatment. The cons from dissolved air flotation and flotation impeller system are the devices tend to have manufacturing and repairing problems and consumption of large amount of energy (Tang and Liu, 2006).

Various studies had been conducted using flotation method. Al-Shamrani, Jamesa and Ziao (2002) carried out a study on dissolved air flotation separation of oil and water. The results pointed out that the oil base can be removed by the flotation method with a pre-treatment using aluminium sulfate for flocculation. In another study, a settling tank simulation was applied (Wang, 2007). The effluent concentration was of 300 mg/L and the minimum has reached 97 mg/L when the concentration of oil was 3000–14000 mg/L. It can be said that the flotation process promoted the degreasing effect. Peeling flotation to carry out refinery wastewater treatment was used by Zhu and Zheng (2002). The results obtained for oil removal rate and suspended solid removal rate were 81.4 % and 69.2 % respectively.

2.1.2 Coagulation

Several studies had been conducted by using the coagulation method. A composite coagulant had used by Lin and Wen (2003) for the treatment of emulsified and dissolved oily wastewater from oil industry. The concentration of the feed was 207 mg/L, whereas the concentration of COD was 600 mg/L. The results showed that the

oil and COD removal efficiency were 98 % and 80 % respectively after the coagulation process by using the composite coagulant.

Zeng et al. (2007) used zinc silicate and anionic polyacrylamide composite flocculants for the treatment of oily wastewater. There was up to 99 % improved oil removal and suspended solids concentration was less than 5 mg/L. However, the drawbacks of this method includes higher capital costs and secondary pollution of water bodies.

2.1.3 Biological Treatment

The use of microorganisms for oily wastewater treatment has bring about some splendid results. Biological method manipulate the usage of microbial metabolism. This method is commonly being employed in activated sludge and biological filter (Kriipsalu et al., 2007; Sirianuntapiboon and Ungkaprasatcha, 2007).

An up flow anaerobic sludge blanket (UASB) coupled with immobilized biological aerated filters (IBAFs) was used by Liu et al. (2013) to treat heavy oil wastewater with large amounts of dissolved recalcitrant organic compounds and low content of nitrogen and phosphorus nutrients. The system was operated for 252 days which includes the start-up of 128 days. The results indicated that the COD, ammonia nitrogen and suspended solid (SS) in the wastewater were decreased by 74 %, 94 % and 98 %, respectively. Analysis from the results showed that most of the alkanes were degraded by the UASB process, while the contribution of I-BAF was in degrading organic compounds and in removing suspended solid.

The performance of Yarrowia lipolytica W29, an oleaginous yeast was examined, which was immobilized by calcium alginate to degrade oil and chemical oxygen demand (COD) (Wu, Ge and Wan, 2009). The oil removal ability of immobilized cells was steady after storing at 4 °C for 30 days and reuse for 12 times and the COD removal rate of immobilized cells was 82%. The results recommended

that immobilized Y. lipolytica has the potential to be a candidate for oily wastewater treatment system.

Recent studies in this area have evidenced promising result. However, the system has challenges in practical application due to the characteristics and performance of microbes under different surrounding conditions. It is hard to meet the requirements according to the new regulations and standards for many industries in disposal of oily wastewater. Hence, it results in increased industrial pollution burden and highlighted environmental pollution problems (Wenyu, Linlin and Luhua, 2013). Nevertheless, biological treatment is generally effective in highly dilute oil-contaminated wastewaters.

2.1.4 Membrane Separation Technology

The simplest way to define membrane filtration is the process of segregating one flow of feed into two streams, where one stream will be more concentrated than the other (Wang et al., 2012). Pressure is used in this process to selectively allow material through a semi-permeable membrane. This principle is also known as the selective permeation. The streams that had been separated can further undergo processing or it can be sent to the suitable outlet in the case of waste stream (Klaysom et al., 2013). A membrane system is an appropriate candidate to be used to acquire a more purified product. It has the ability to filter particulates from the dissolved species and segregating dissolved species themselves. On top of that, the process of filtration can hinder dissolved species of certain sizes from passing through the membrane while providing passage for other components to permeate through the membrane with the proper membrane selection. This mechanism is known as the size exclusion principle (Phao et al., 2013).

The selection of membrane depends upon several criteria including the type of the feed solution, parameters during the operation such as pressure and temperature, type of application and separation goals on what kind of material to be filter out (Morillo et al., 2014; Krishna, 1989). Organic and inorganic membranes are the two

types of membranes available and both have their own advantages and disadvantages. It is important to determine what type of membrane is most relevant for the application (Synderfiltration, 2017).

There are few different types of membrane materials such as polymeric, ceramic and metallic. Although ceramic, metallic and several other types of materials may be available, the majority of membranes used commercially are made from polymer. Polymeric material is being favoured due to the fact that it is lower in cost than membranes constructed of other materials (Dickhout et al., 2016). Polymeric membranes consist of natural and synthetic polymers and both types of polymer membranes are categorized as organic membrane. Polytetrafluoroethylene (PTFE), polysulfone, and polyvinylidenedifluoride (PVDF) are some famous synthetic polymers while rubber, cellulose and wool are example of natural polymers.

Inorganic membranes consist of ceramic and metallic membranes. Ceramic membranes are made from metal (aluminium or titanium) and non-metal (oxides, nitride, or carbide) materials. Due to inertness and resistance of fouling and chemical attack, ceramic membranes are commonly used in acidic or basic environments. The potential of membrane cracking due to its high sensitivity to temperature and the relatively higher cost are the disadvantages of ceramic membranes. The downside for metallic membranes is the poisoning of surface effect. Despite the cons, inorganic membrane have several pros such as high thermal and chemical stability, inertness to microbiological degradation, and ease of cleaning after fouling. Regardless, majority of membrane is made from polymer because inorganic membranes tend to have higher capital costs due to the necessity of specific thickness to withstand pressure drop differences (Synderfiltration, 2017).

2.2 Membrane Separation Process

There are four main membrane separation processes; microfiltration (MF), ultrafiltration (UF), nanofiltration (NF) and reverse osmosis (RO). RO have the

smallest pore size followed by NF, UF and MF in the increasing order (Morillo et al., 2014).

Microfiltration (MF) membranes commonly used for the filtration of large particulates, colloids and bacteria from feed streams. MF membranes have pore sizes ranging from 0.1 to 10 μm. This membrane is well-known in the food and beverage industry for treating wastewater before discharging it to a municipal sewer (Macedonio et al., 2012).

The process of ultrafiltration (UF) is very much similar to microfiltration, except that UF membrane has smaller pore sizes ranging from 0.01 to 0.1 μm. The application of UF membranes includes eliminating viruses and polypeptides (Pendergast and Hock, 2011).

Nanofiltration (NF) membranes are much more alike reverse osmosis membranes in the terms that they contain a thin-film composite layer (<1 μm) and porous layer (50 to 150 μm). The pore sizes ranging from 0.001 to 0.01 μm. NF membranes filter out multivalent salts and uncharged solutes, while selectively allow some monovalent salts to pass through (Dickhout et al., 2016). In addition, residual natural organic matter from drinking water can be removed through NF membranes (Matilainen, 2004).

Reverse osmosis (RO) membranes pores are even smaller than nanofiltration membranes where the pore sizes ranging from 0.0001 to 0.001 μm. They could remove all monovalent ions while allowing permeation of water molecules. They can also reject viruses and bacteria present in feed solutions. RO is generally used for seawater desalination (Dickhout et al., 2016).

Table 2.1 shows the membrane separation process and its application while Figure 2.1 shows the membrane separation process and its product. The objectives of the development of these technologies are to establish filtration process with low operation cost and high efficiency (Morillo et al., 2014; Krishna, 1989).

Table 2.1: Membrane Separation Process and its Application (Pendergastet and Hock, 2011).

Technologies	Application
Microfiltration	Separation of suspended solids, protozoa and bacteria
Ultrafiltration	Separation of virus and colloid
Nanofiltration	Separation of heavy metals and dissolved organic compounds
Reverse Osmosis	Water reuse; Separation of dissolved salt and ions

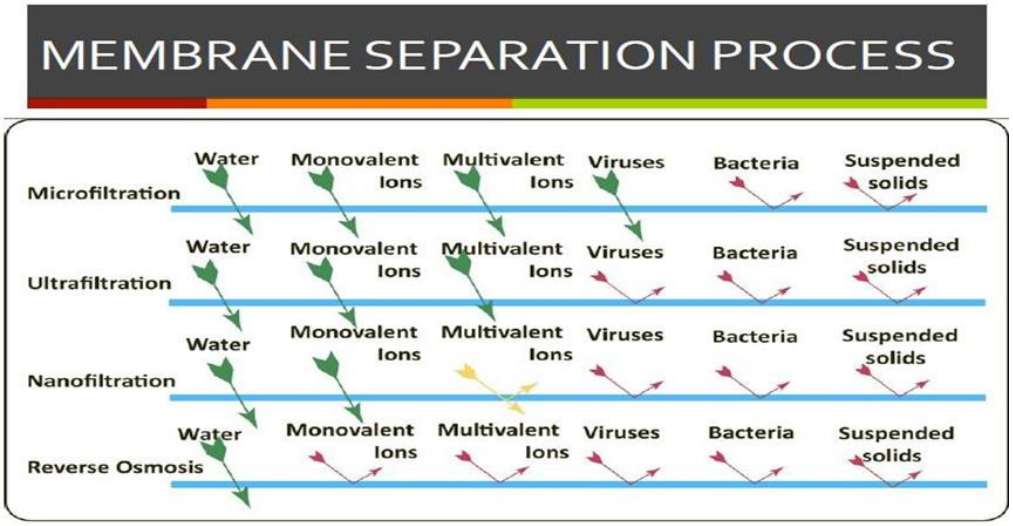

Figure 2.1: Membrane Separation Processes and Separation Products (Macedonio et al., 2012).

2.3 Review on Membrane Filtration for Oily Wastewater Treatment

Membrane filtration has been widely used for oily wastewater treatment currently. Various researchers investigated the performance of membrane in the filtration of pollutants from oily wastewater (Jamaly, Giwa and Hasan, 2015; Yu, Han and He, 2013).

Research on five types of polymeric membranes and its performance in treating industrial oily wastewater was conducted by Salahi et al. (2013). The membrane consisted of two microfiltration membranes: polysulfone (PSF) (0.1 μm) and PSF (0.2

μm) and three ultrafiltration membranes: polyacrylonitrile (PAN) (20 kDa), PAN (30 kDa), and PAN (100 kDa). The data obtained highlighted that PAN (100 kDa) had the best performance than other membranes. PAN (100 kDa) has ability to remove 97.2 % oil and grease content, 94.1 % total suspended solids and 31.6 % total dissolved solids. In addition, the membrane showed permeation flux of 96.2 L/ (m^2•hr) and has declined fouling resistance up to 60 %.

Salahi et al. (2013) did another research that focused on a sheet nanoporous membrane. PAN used in the filtration of oily wastewater. The findings showed that the rejection of suspended solids, total dissolved solids, oil and grease content, COD and BOD are improved to 100 %, 44.4 %, 99.9 %, 80.3 % and 76.9 % respectively.

Asatekin and Mayes (2009) had declared that combination of polyacrylonitrile and polyacrylonitrile-graft-poly (ethylene oxide) membrane has capability to filter dispersed and free oil efficiently rather than polyacrylonitrile membrane alone. From the study, the oil rejection rate obtained is 96 %. Furthermore, the blended membrane showed better resistance towards fouling.

A low-cost, hydrophilic ceramic/polymeric composite membrane from clay, kaolin and a small amount of binding materials was prepared by Mittal (2013) for the treatment of oily wastewater. It was found that higher flux decline was resulted due to higher pressure and higher initial oil concentration. Rejection was noticed to be increased with time. 93 % was the maximum rejection that found.

Zhang et al. (2009) had conducted study by adding microcrystalline cellulose (MCC) to a polysulfone (PSF) membrane to treat oily wastewater. The results from the study revealed that the oil retention is 99.16 % and the total oil content in the permeation is 0.67 mg/L and has met the requirement for discharge (<10 mg/L). The membrane showed permeation flux of 234.2 L/ (m^2•hr). It can be assumed that the PSF composite membranes are resistant to fouling and can be used in oily wastewater treatment.

Yan et al. (2009) employed polyvinylidenedifluoride (PVDF) and aluminium oxide nanofiller to prepare a nanocomposite membrane. It is proven that the nanocomposite membrane have better water permeation compared to pure PVDF membrane based on the results obtained. Moreover, the membrane also had better oil rejection rate, total organic compound retention, suspended solid retention as well as COD retention. The results showed that the membrane has ability to maintain its performance in terms of rejection rate and permeation flux after washing. This validated that aluminium oxide nanofiller increases properties of anti-fouling and enhances the hydrophilicity of the membrane.

Yi et al. (2011) explored PVDF membrane modified using nanosized titanium oxide/aluminium oxide for separation of water/oil emulsion. The research indicated that modified membrane exhibited higher relative flux and better antifouling property due to the enhanced hydrophilicity. The flux recovered about 94 % after washing with pure water and it is higher than pure PVDF that obtained only 88 % flux recovery after washing which was the highlight of this study. The modified membranes had 100 % flux recovery whereas pristine PVDF membrane only has 95 % flux recovery when washed with sodium hypochlorite. This demonstrates that addition of titanium oxide/aluminium oxide nanomaterial enhances the potential of using PVDF membrane in oily wastewater treatment.

Zhang et al. (2014) added phosphorylated silica nanotubes (PSNTs) into PVDF membrane matrix. The objectives of the research were to study the flux behaviour versus time, temperature and pressure. The casted membrane was able to achieve about 96 % of oil rejection and showed better anti-fouling properties. The membrane have shown only a slight decline in permeation flux through different physical and chemical cleaning methods. The membrane showed permeation flux of between 220 and 245 L/ (m^2•hr) after physical cleaning and the permeation flux has declined to between 160 and 180 L/ (m^2•hr) through chemical cleaning.

2.4 Membrane Separation Technology Limitations

Majority of membranes used commercially are made of polymeric material. The benefits of this membrane are that it does not need secondary processes to aid in filtration or any chemical and energy input. This helps to save the capital cost. Nonetheless, membrane fouling is unavoidable during membrane filtration processes. It had been stated in various studies that one of the main reasons for fouling is intrinsic hydrophobicity of membrane. This situation leads membrane system to operate at high power to ensure a continuous capacity of the membranes (Qu, Alvarez and Li, 2013). At one point the pressure will upswing too much due to the fouling that it is no longer economically and technically culpable (Wang et al., 2013).

Fouling is the main operating issue especially in treating oily wastewater. Fouling leads to high energy consumption and it will also reduce the lifespan of membrane (Qu, Alvarez and Li, 2013). Breakdown of the membrane fibres can be caused by high pressure and extended operation time of membrane (Peng et al., 2009). These drawbacks will increase the maintenance and operation cost. In addition, another common limitation is the trade-off between the membrane selectivity and water flux. Fouling causes decline in permeation flux, change in selectivity and separate ability during filtration operation. An ideal membrane must have high water flux and high solute rejection. Moreover, it also must have high stability to prevent fouling and reduce cost as well as producing water with higher level of purity (Gryta, Karakulski, and Morawski, 2001; Yang et al., 2011).

A study conducted by Wang et al. (2012) has revealed the potential of PVDF membrane to be can used in oily wastewater filtration. Despite the revelation in this research, the membrane was found to be unsuccessful to be reused. The membrane could not be regenerated using conventional cleaning method. Asatekin and Mayes (2009) stated that although ultrafiltration method shows potential in oily wastewater treatment, the application is very restricted due to the fouling of the membrane.

In general, fouling can hit any type of membrane regardless the material the membrane is made of. The main four types of fouling are scaling, silting, bacteria fouling and fouling due to organic material. Fouling by silting, bacteria and organics

such as oil is generally overcome by an appropriate pre-treatment procedure. Common sources of fouling are silt due to organic compounds, corrosion products, and fine salts particulate depositing on the membrane pore surface. Biological fouling takes place due to build-up of biofilms of extracellular polymeric substances, microbial cells matrix and biological matter on the membrane surface. Organic fouling is the accumulation of material such as oil onto the membrane surface and it will end up in clogging the pores which eventually form a cake layer over time. This type of fouling is common in membrane filtration processes (Sun et al., 2014).

2.5 Graphene Oxide (GO)

Graphene oxide (GO) is a single atomic layered material produced from exfoliation of graphite oxide (Yang et al., 2009). Graphite oxide can be easily produced by exhaustive oxidation of graphite crystals using strong mineral acids and oxidizing agents (Dreyer et al., 2009). Graphite consists of graphene layers aligned in AB stacking sequence. The distance between the layers kept constant about 0.34 nm by Van der Waals forces (Ciszewski and Mianowski, 2013). Chemical oxidation of graphite involves intercalation of a wide range of oxygen-containing chemical functionalities in the interlayer space that disrupts the delocalised electronics structure of graphite layers (Potts et al., 2011). This breaks the Van der Waals forces which hold the layers and increase the distance between the layers (Ciszewski and Mianowski, 2013). The oxygenated graphite solids are then hydrolysed and rinsed with water. Solid graphite oxide is recovered by drying. The drying process can be done in atmospheric pressure or vacuum at room temperature. It can be heated in air at low temperatures (50-65 ºC) alternatively, to eliminate thermal decomposition. Normally, some residual water is present in the solid obtained due to the low drying temperature. Graphite oxide can then be readily exfoliated into GO nanosheets (Li et al., 2014).

GO is similar to a graphene sheet structurally. The structure of GO is as shown in Figure 2.2. GO contains a range of functional groups containing oxygen; hydroxyl and epoxide in the basal planes and carboxyl groups at edges of plane compared to graphene (Sengupta et al., 2011). The GO sheets consist of both aromatic regions

containing unoxidized benzene rings and aliphatic regions with oxidized six-carbon rings where oxygen-containing groups attach to. The carbon-oxygen bonds cause partial change of carbon atoms hybridization from sp^2 to sp^3 which leads to the insulating property of GO (Bykkam et al., 2013). GO is able to disperse in water and at the same time maintain its suspensibility in organic solvents since the oxygen-containing functional groups have high affinity to water molecules (Paredes et al., 2008). Stirring and sonication of GO in solvents further enhance the dispersions of graphene oxide fillers (Zhu et al., 2010). The oxygen-containing groups in GO attribute to better adhesion and improved mechanical interlocking with the polymer chains (Ramanathan et al., 2008).

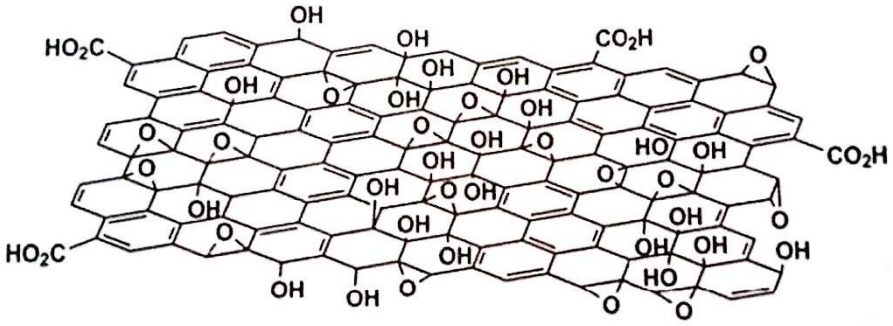

Figure 2.2: Structure of GO (Dreyer et al., 2009).

GO is commonly “reduced” by thermal annealing or chemical reducing agents to partially restore some of the electrical, mechanical as well as thermal properties of the pristine graphene (Raidongia, Tan and Huang, 2014). Several literatures have reported the chemical production of graphene from GO. The oxidation of graphite crystal with strong oxidizing agents is followed by thermal or ultrasonic treatment to remove the functional group in order to obtain the graphene sheet. This method can give a very high production of graphene and improve the compatibility of matrix composite by introduction of functional groups in the oxidation process (Park and Ruoff, 2009; Zhu et al., 2010).

GO itself exhibits many fascinating properties. It seems to fit into the categories of soft material such as a liquid crystal, membrane, anisotropic colloid, two-dimensional (2D) polymer or amphiphile (a chemical compound obtaining both

hydrophilic and lipophilic properties) (Raidongia, Tan and Huang, 2014; Cote, Kim and Huang, 2009). In addition, the active sites were provided by the functional groups for additional chemical modification for instance functionalization (Dreyer et al., 2009). Additionally, graphene oxide can be easily dispersed in water and organic solvents due to the presence on oxygenated group in its structure. It is an advantage because it can be mixed with any matrixes to improve their electrical, chemical and mechanical properties (Cui, Kundalwal and Kumar, 2016; Wilkinson, 2017; Macedonio et al., 2012).

2.6 Structural Models of GO

Few structural models have been proposed for GO since its discovery by Brodie in 1859. Many earliest structural models suggested that GO was composed of regular lattices with distinct repeat units. Structure proposed by Hofmann and Holst comprised of epoxy groups scattered on the basal planes of graphite where oxygen is bound to the carbon atoms of the hexagonal layer by epoxide linkages. Figure 2.3 Displays Hofmann and Holst's Model. This gives the GO a net molecular formula of C_2O (Hofmann and Holst, 1939). Ruess (1946) who took into account of the hydrogen content of GO, proposed a slightly different model which included hydroxyl groups on the basal plane other than epoxy groups illustrated in Figure 2.4. This model also indicates that the carbon atoms in the basal plane of GO is sp^3 hybridized rather than the sp^2 hybridized in Hofmann and Holst's model.

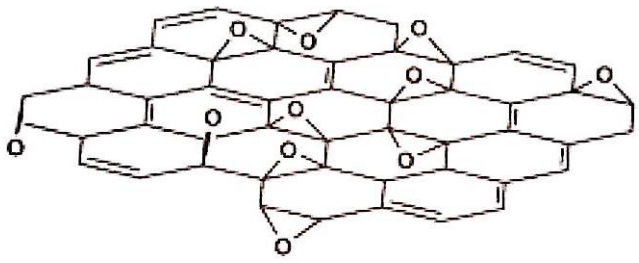

Figure 2.3: Hofmann and Holst's Model (Dreyer et al., 2009).

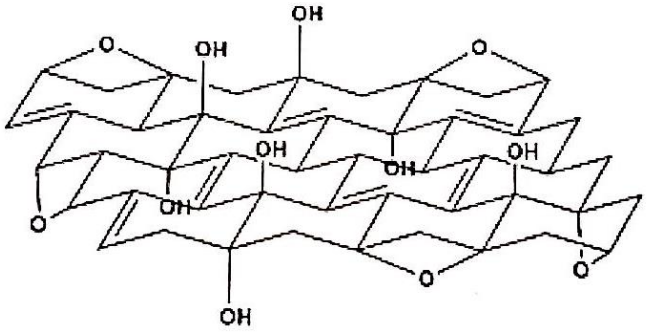

Figure 2.4: Ruess's Model (Dreyer et al., 2009).

Then, Scholz and Boehm (1969) suggested a model which contains neither of the epoxide nor ether groups as provided in Figure 2.5 This model composes of regular quinoidal species and conjugated carbon backbone. Another model by Nakajima and Matsuo (1988) as shown in Figure 2.6 suggested that two carbon layers link to each other by sp^3 C-C bonds perpendicular to the layers. This model stressed on the interactions of the hydroxyl and carbonyl groups between the sheets. They observed the changes in the interlayer spacing in GO with humidity and argued that it can be directly related to the ratio of hydroxyl to carbonyl groups which ranges from a completely dehydrated C_8O_2 to structure dominated by hydroxyl group $C_8(OH)_4$.

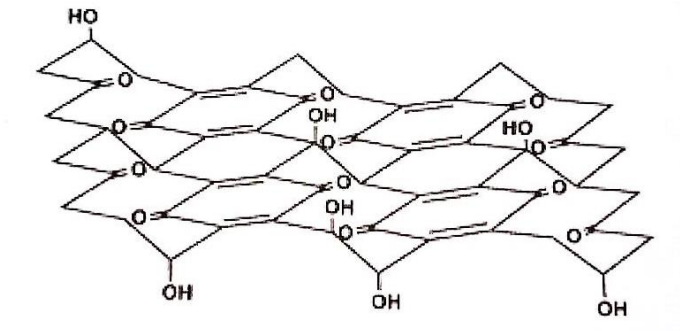

Figure 2.5: Scholz and Boehm's Model (Dreyer et al., 2009).

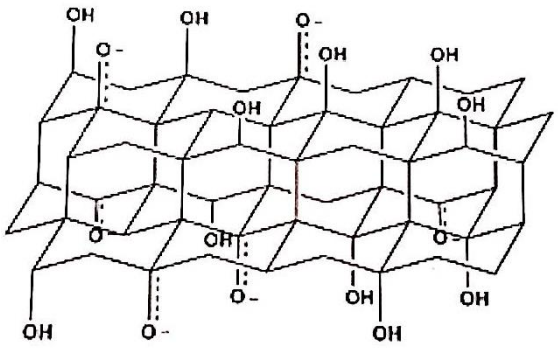

Figure 2.6: Nakajima and Matsuo's Model (Dreyer et al., 2009).

The actual chemical structure of the GO has been under debate due to the complexity of the material and lack of precise characterization techniques (Dreyer et al., 2009). The most well-known model of the recent ones was proposed by Lerf and Klinowski as illustrated in Figure 2.7 although there has been updated structure from Gao et al. (2009). The model is based on the random distribution of aromatic regions of unoxidized benzene rings and regions with aliphatic six-member rings where the oxygen functionalities such as epoxides, carbonyl, carboxyl and hydroxyl groups attach to. Lerf and Klinowski found that epoxy and hydroxyl groups were usually located fairly close to each other by Nuclear Magnetic Resonance (NMR) analysis. Modern models and experimental measurements of GO indicates a random distribution of functional groups similar to Lerf and Klinowski model (Raza, 2012). Observation under high-resolution transmission electron microscopy (HRTEM) supports the Lerf and Klinowski model (Erickson et al., 2010).

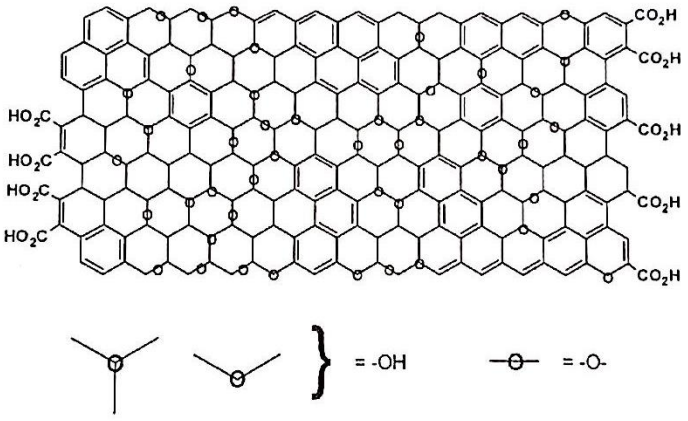

Figure 2.7: Lerf and Klinowski Model of GO (Dreyer et al., 2009).

Regardless of to which model is accurately representing the structure of GO, the presence of oxygen functionalities enables it to interact with hydrophilic polymers as well as aqueous and non-aqueous solvents for wider applications.

2.7 Morphological State of GO in Polymer Matrix

Graphite oxide has a layered structure resembling certain silicates which have been extensively studied as composite fillers (Paul and Robeson, 2008). Previous studies on nanoclay-based composites suggested three common platelet dispersion states namely stacked, intercalated, or exfoliated for layered structure nanofillers as represented in Figure 2.8. In fact, similar dispersion pattern of graphene-based fillers in polymer matrix has been observed in both graphene nanoplateles (GNP) and GO-based polymer nanocomposites (Potts et al., 2011).

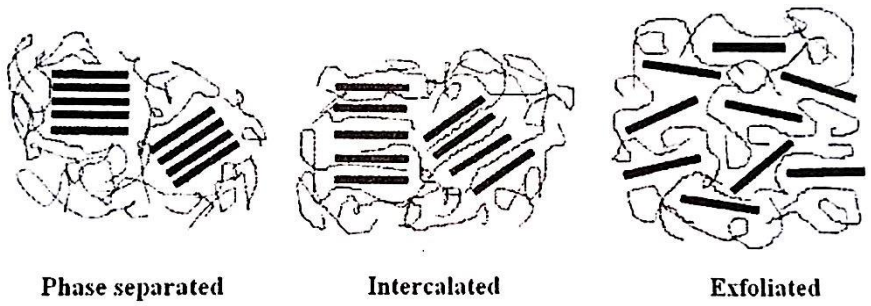

Figure 2.8: Morphological States of Graphene-based Nanocomposites (Wang, Yan and Ma, 2012).

Graphite oxide has to be exfoliated so that the graphene oxide sheets are well dispersed in the polymer matrix to enhance the mechanical properties of GO/polymer nanocomposites effectively (Thostenson, Li and Chou, 2005). An exfoliated graphite oxide has a higher aspect ratio in contrast to either intercalated or stacked state (Fu and Qutubuddin, 2001).

2.8 Preparation of GO

The preparation of GO involves two basic steps which are graphite powder is oxidized to graphite oxide and followed by exfoliation of graphite oxide into graphene oxide (GO). Figure 2.9 demonstrates the two steps of preparing graphene oxide (GO) from graphite.

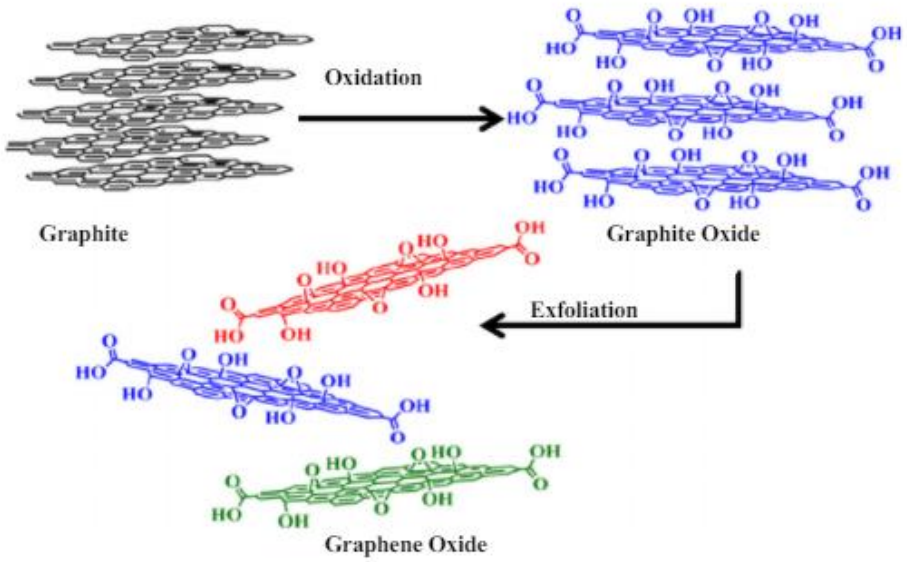

Figure 2.9: The two steps of preparing graphene oxide (GO) from graphite (Ammar et al., 2015).

2.8.1 Chemical Route Preparation of Graphene Oxide

Graphite oxide can be synthesized by referring to the method developed by Brodie, Staudenmaier and Hummers-Offeman. The procedure in the synthesis process includes oxidation of graphite with strong acid and oxidizing agent together with the hydrolysis process, washing, centrifuging and drying (Marcano et al., 2010).

In year 1859, B. C. Brodie, a British chemist produced the very first graphite oxide through synthesis using potassium chlorate ($KClO_3$) to graphite slurry in fuming nitric acid (HNO_3) during the research on the structure of graphite (Marcano et al.,

2010). The oxidation was repeated for another three times until the oxygen content reached the maximum. After completion of oxidation process, the net empirical formula of the graphene was then found to be $C_{2.19}H_{0.80}O_{1.00}$ (Dreyer et al., 2009).

Nearly 40 later, L. Staudenmaier slightly improved Brodie's method. Staudenmaier's method was found to enhance the safety of experiment and reduce the footprint of harmful and toxic gas (Shao et al., 2012). Over the course of reaction, Staudenmaier did modification on the method by dividing the chlorate to multiple portions and adding them one after another. Concentrated sulphuric acid was also added to increase the acidity of the mixture. This modification seems to be viable as the reaction can be carried out in solely in reaction vessel (Dreyer et al., 2009).

However, both Staudenmaier and Brodie's method and procedures have a common thing which is the choice of using nitric acid and potassium chlorate as oxidizing agents (Shao et al., 2012). The reason behind their choice is the nature of nitric acid which tends to react strongly with aromatic carbons and the properties of potassium chlorate as a strong oxidizing agent. Potassium chlorate is also commonly used in preparation of explosive materials (Dreyer et al., 2009). The oxidation processes involving potassium chlorate are vigorous which may result in spontaneous ignition or explosion (Wu and Ting, 2013).

Afterwards, Hummers and Offeman advanced a new method of oxidation of graphene. They utilized the combination of potassium permanganate ($KMnO_4$) and concentrated sulphuric acid (H_2SO_4) as oxidizing agents. This method also includes the use of sodium nitrate. Hydrogen peroxide is added to the diluted mixture after oxidation step to reduce the manganese. The active species in permanganate in this method is diamanganese heptoxide (Mn_2O_7). Figure 2.10 shows the formation of diamanganese heptoxide from potassium permanganate.

$$KMnO_4 + 3H_2SO_4 \rightarrow K^+ + MnO_3^+ + H_3O^+ + 3HSO_4^-$$
$$MnO_3^+ + MnO_4^- \rightarrow Mn_2O_7$$

Figure 2.10: Formation of Diamanganese Heptoxide (Mn_2O_7) from Pottasium Permanganate ($KMnO_4$) in the Presence of Strong Acid (Dreyer et al., 2009).

These three reactions achieve similar levels of oxidation where ratio of carbon to oxygen is approximately 2:1 (Staudenmaier, 1898). Hummers method takes the shorter time to produce GO when compared with Brodie and Staudenmaier method. Furthermore, it is less hazardous than the other two methods. In spite of slightly modified versions developed over the years, these three methods comprise the primary routes for producing GO.

2.8.2 Exfoliation of Graphite Oxide

Two common techniques for exfoliation of graphite oxide are solvent exfoliation and thermal exfoliation. Graphite oxide is exfoliated by ultrasonication or mechanical stirring in water or polar organic solvents in solvent exfoliation. This form colloidal suspensions of GO (Potts et al., 2011). Sonication process may lead to fragmentation of the platelets and reduction of their lateral dimension. Mechanical stirring is able to produce GO platelets of larger lateral dimensions but in a very slow way along with low yield (Paredes, Villar-Rodil, Martinez-Alonso and Tascon, 2008).

2.9 Properties and Applications of Nitrile Butadiene Rubber (NBR)

NBR basic building block consists of the family of unsaturated copolymers of butadiene monomers. Its features generally rely on the composition of nitrile within the NBR polymer, which plays a major role in the chemical and oil resistant of NBR. The flexibility tends to be reduced despite the higher nitrile content that enhances the

oil, abrasion and heat resistance within the polymer. Therefore, the right composition is vital for the needed products. In addition, NBR also has incredible elongation properties along with compressibility and tensile strength (Hanhi, Poikelispaa and Tirila, 2007).

The most familiar type of nitrile rubber with acrylonitrile (ACN) content of 31–35 % has the ability to endure temperature ranging approximately from -40 to 107 °C. NBR can be considered to be the main oil, fuel, and heat resistant elastomer in the world. It also has good resistant properties towards aliphatic hydrocarbons. Nevertheless, the limitation of NBR is that it has weaker resistance to ozone, sunlight and weathering (Hanhi, Poikelispaa and Tirila, 2007).

Nitrile rubber finds its uses in automotive industry as sealant and gaskets, which will be exposed to oils in high temperature. Besides that, it is also used in application such as automotive water handling and in fuel and oil handling hose. Moreover, NBR is also widely preferred in healthcare sector. NBR is a suitable candidate for the production of protective gloves due to its properties. Some other applications of nitrile rubber includes for hoses that are hydraulic, for producing belts used in conveyer and for sealants used in plumbing, oil column gaskets and many more (Mackey and Jorgensen, 1999). Furthermore, due to its ability to endure a range of temperature from as low as -40°C to merely 108°C, NBR is deemed to be a good choice for footwear, foams, and moulded goods (Nitrile Rubbers, 2017).

CHAPTER 3

METHODOLOGY

3.1 Introduction

This chapter covers on the raw materials used for the synthesis of graphite oxide and the NBR latex and NBR latex /GO membranes preparation, supplier names, physical properties of the raw materials, synthesis of graphite oxide, exfoliation of graphite oxide, latex compounding method, degasification method, membrane casting and curing conditions. Furthermore, characterization and testing methodologies of the membrane were explained. The overall experimental design is shown in Figure 3.1.

3.2 Experiment Flow Chart

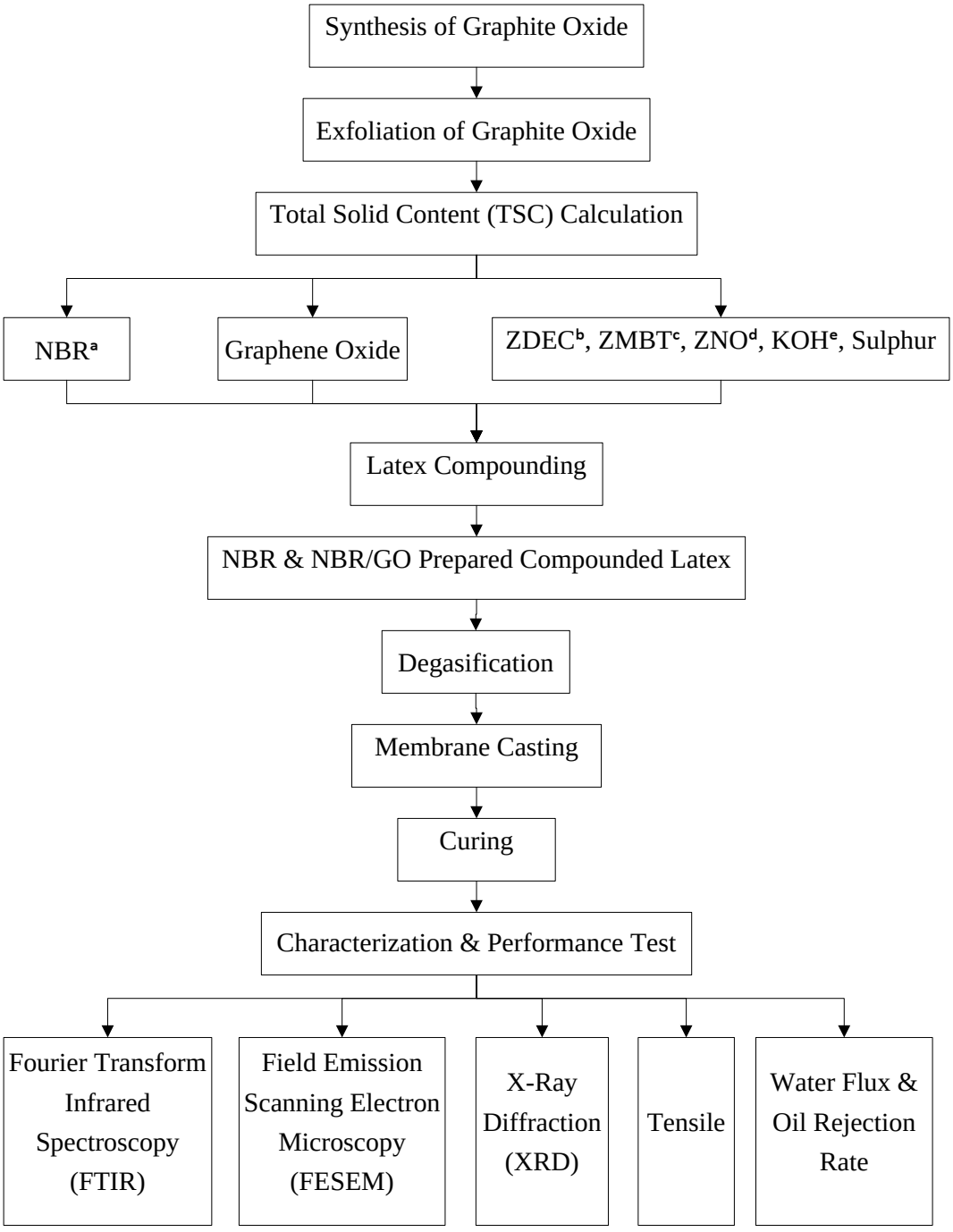

a = Nitrile Butadiene Rubber
b = ZincDiethyldithiocarbamate
c = Zinc 2-Mercaptobenzothiazole
d = Zinc Oxide
e = Potassium Hydroxide

Figure 3.1: Overall Flow of Methodology.

3.3 Raw Materials

Graphite oxide was prepared from graphite nanofibre (GNF). GNF was supplied by Platinum Senawang Sdn Bhd. Sulphuric acid (H_2SO_4, 95-97 %) and hydrochloric acid (HCl, 37 %) were provided by QRëC® Sdn Bhd while hydrogen peroxide (H_2O_2, 30-31 %) was purchased from SYSTERM® ChemAR®. Potassium permanganate ($KMnO_4$, 99 %) was obtained from Bendosen Laboratory Chemicals and sodium nitrate ($NaNO_3$, 99 %) was supplied by GENE Chem. Deionized water was obtained from the laboratory. Anodisc membrane used for filtration was bought from Whatman Inc.

Nitrile butadiene rubber (NBR) was obtained from Synthomer Sdn Bhd with total solid content (TSC) of 62.39 %, pH value of 8 and viscosity of 23 mPa.s.

Latex compounding ingredients which are zinc diethyldithiocarbamate (ZDEC), zinc 2-mercaptobenzothiazole (ZMBT), zinc oxide (ZNO), potassium hydroxide (KOH), and sulphur were all purchased from Zarm Scientific & Supplies Sdn Bhd Malaysia. The functions of each compounding ingredient are listed in Table 3.1.

Table 3.1: Functions of Compounding Ingredients.

Compounding Ingredients	Function
Sulphur	Cross-linking agent
Zinc Oxide	Activator of vulcanisation
ZDEC	Accelerators
ZMBT	Accelerators

For oily wastewater preparation, diesel was purchased from BHP gas station located at Mambang Diawan, Kampar, Perak. Sodium dodecyl sulphate (SDS) was obtained from System Company.

3.4 Synthesis of Graphite Oxide

Graphite oxide was produced using the conventional Hummers method. A 500 ml beaker filled with 115 ml of H_2SO_4 was placed under an overhead mechanical stirrer model IKA RW 20 Digital for stirring at 400 rpm. An ice bath was used to maintain the temperature of the content in the beaker at 0 °C. Then, 5 g of GNF followed by 2.5 g of $NaNO_3$ were added into the beaker. After $NaNO_3$ was dissolved, 15 g of $KMnO_4$ was added slowly into the beaker to maintain the temperature below 30 °C. Visible green suspension was formed almost instantaneously.

After stirring for 10 minutes, ice bath was removed and the temperature was brought up to 35 °C. The solution was then stirred vigorously at 500 rpm for duration of 3 hours at room temperature. After 3 hours, the stirring speed was reduced to 400 rpm and 230 ml of deionized water was added slowly into the solution. As water was added, the temperature of the mixture increased to 70 °C and this temperature was maintained. The solution was continued to be stirred for 10 minutes. Then, the solution was poured into 700 ml of deionized water. 12 ml of H_2O_2 was added to reduce the residual $KMnO_4$, resulting a light yellow suspension. The mixture was then left overnight and filtered using Whatman Anodisc membrane.

The filtered cake was first washed with 5 % HCl solution, followed by filtration with Whatman Anodisc membrane and then washed with the deionized water. The solution was centrifuged in a centrifuge machine model Velocity 14R for 30 minutes at the speed of 14 000 rpm under room temperature. The supernatant was decanted after measuring its pH. Filtration, washing and centrifugation were repeated until the pH of supernatant fell into the range 5-7. The precipitate dispersed in deionized water and dried in oven model UNB 500 overnight at 60 °C.

3.5 Exfoliation of Graphite Oxide

The graphite oxide was exfoliated into graphene oxide (GO) by ultrasonication. Ultrasonication process was carried out by the use of a probe-type ultrasonic homogenizer. Mixing ratio of graphite oxide to distilled water was fixed to 1:3. Thus, according to the mixing ratio, the dry weight of graphite oxide was added to appropriate amount of distilled water in a beaker and it was mixed well by using a spatula. Then, the beaker was placed in the probe-type ultrasonic homogenizer for 30 minutes. Figure 3.2 shows the ultrasonication process of graphite oxide using a probe-type ultrasonic homogenizer. After 30 minutes, the beaker was removed from the ultrasonic homogenizer and the mixture was ready to be used.

Figure 3.2: Sonication of Graphite Oxide.

3.6 Preparation for Latex Compounding

3.6.1 Total Solid Content (TSC) Calculation

Before the compounding process, the total solid content (TSC) of each material was calculated. An evaporating dish was labelled accordingly for each ingredient. The weight of each evaporating dish was recorded (W1). Next, roughly 2 grams (initial weight) of each material which are NBR, ZDEC, ZMBT, ZNO, KOH, sulphur, and graphene oxide were placed in the respective evaporating dish and subsequently placed in the oven model UNB 500 at 105°C for 2 hours.

After 2 hours, the evaporating dishes were removed from the oven and placed under the room temperature for 15 minutes. The weights were measured and recorded after 15 minutes. Next, all the dishes were placed back in the oven for 15 minutes at 105°C and removed again after 15 minutes. After cooling down at room temperature, the weights were measured and recorded. The steps were repeated until constant weight was reached. The final constant weight was recorded (Sarvini, 2017). TSC was calculated using Equation 3.1.

$$TSC = \frac{Dry\ sample\ (Final\ weight)}{Initial\ sample\ (Initial\ weight)} \times 100\ \% \tag{3.1}$$

After the TSC calculation, the real compound weights of each ingredient were calculated using Equation 3.2 to 3.7 as follows:

$$Real\ weight_{NBR} = x\ g \tag{3.2}$$

$$Dry\ weight_{NBR} = \frac{TSC}{100} \times Real\ weight_{NBR} \tag{3.3}$$

$$100\ phr = Dry\ weight_{NBR} \tag{3.4}$$

$$1\ phr = \frac{Dry\ weight_{NBR}}{100} \tag{3.5}$$

$$Dry\ weight\ = \frac{Dry\ weight_{NBR}}{100} \times formulation \quad (3.6)$$

$$Real\ weight = Dry\ weight\ \times \frac{100}{TSC} \quad (3.7)$$

3.6.2 NBR and NBR/GO Compounding

Pure NBR membrane was prepared to highlight the contribution of GO in membrane performance. NBR latex used for this research was compounded using an overhead mechanical stirrer model IKA RW 20 Digital. Firstly, the NBR latex was stirred with half amount of the KOH at 200 rpm, then followed respectively by the other compounding ingredients (ZNO, ZDEC & ZMBT). The compounding formulation reference was based on the research done by Sarvini (2017) and is shown in Table 3.2. Sulphur was added lastly to prevent increment in viscosity as sulphur promotes cross-linking. Another half amount of the KOH was used to rinse the compounding ingredients. Stirring was continued for another 30 minutes at 250 rpm. The pH value was measured during compounding to ensure that the pH value is more than 7 (if the pH value is less than 7, KOH to be added drop by drop until the pH value reach 7).

For the NBR membrane with GO, firstly, the NBR latex was stirred with half amount of the KOH at 200 rpm and then, the GO solution was added to NBR followed by the other compounding ingredients (ZNO, ZDEC, ZMBT & sulphur). The stirring speed and time were as same as for compounds without GO. The steps were repeated with different formulation of GO to determine the optimum loading of GO. The compounding formulation is shown in Table 3.3. Figure 3.3 shows the compounding process of NBR and NBR/GO using an overhead mechanical stirrer.

Figure 3.3: Compounding of NBR and NBR/GO.

Table 3.2: Compounding Formulation for Pure NBR Membrane.

Materials	Total Solid Content (%)	Formulation (phr)	Dry weight (g)	Real Compound Weight (g)
NBR	62.39	100.00	62.3900	100.0000
KOH	10.00	1.0	0.6239	6.2390
ZNO	46.81	1.0	0.6239	1.3328
ZDEC	54.87	1.0	0.6239	1.1371
ZMBT	50.57	0.5	0.3120	0.6170
Sulphur	50.64	1.0	0.6239	1.2320

Table 3.3: Compounding Formulation for NBR/GO Membrane.

Materials	Total Solid Content (%)	Formulation (phr)	Dry weight (g)	Real Compound Weight (g)
NBR	62.39	100.00	62.3900	100.0000
KOH	10.00	1.0	0.6239	6.2390
ZNO	46.81	1.0	0.6239	1.3328
ZDEC	54.87	1.0	0.6239	1.1371
ZMBT	50.57	0.5	0.3120	0.6170
Sulphur	50.64	1.0	0.6239	1.2320
GO	24.55	0.5	0.3120	1.2709
		1.0	0.6239	2.5413
		1.5	0.9359	3.8122
		2.0	1.2478	5.0827

3.7 Preparation of Membrane

3.7.1 Degasification

Degasification was carried out in a vacuum drying oven model TVAC-53 to remove the excess bubbles or entrapped air in the compounded latex. The compounded latex was placed in the vacuum drying oven and the temperature was set to room temperature while the pressure was set to vacuum condition (0.06 MPa) for 15 minutes.

3.7.2 Casting of Membrane

After degasification, the NBR and NBR/GO compounded latex was used to cast the membrane using a membrane auto casting machine from Autonics Corporation.

Figure 3.4 shows the setup of the membrane auto casting machine for the preparation of membrane.

The casting knife was fixed with a gap of 0.05 mm and was placed on the glass plate and in front of the moving beam. The compounded latex was then poured evenly onto the glass plate and was cast using the casting knife. The speed of the moving beam was fixed at 150 rpm and the process distance was set to 220 mm. The compounded latex was swept on the top of the glass plate and the casting film formed uniformly. Then, the membrane auto casting machine was switched off. After 15 minutes under room temperature, the glass plate was placed into the drying oven model UNB 500 as shown in Figure 3.5 at 100 °C for two different curing times, which were 2 hours and 3 hours for curing purposes. Two different curing times were set to find out the optimum curing time for NBR and NBR/GO membrane.

Figure 3.4: Membrane Auto Casting Machine Setup.

Figure 3.5: Curing Process in Drying Oven.

3.8 Characterization

3.8.1 Fourier Transform Infrared Spectroscopy (FTIR)

FTIR was carried out using PerkinElmer Spectrum ex1 to identify the types of chemical bonds and functional groups in GNF, graphite oxide, NBR and NBR/GO membranes. The analysis was carried out to determine the absorption band at the wavelength between 4000 cm^{-1} to 400 cm^{-1} with 4 scans at a resolution of 4 cm^{-1}. For GNF and graphite oxide, the samples are prepared with KBr. For NBR and NBR/GO membranes, it was used directly by cutting it down into smaller size since the samples were in film form. Background spectrum was captured before samples were scanned.

3.8.2 Field Emission Scanning Electron Microscopy (FESEM)

Morphology of the NBR and NBR/GO membranes at magnification of X200, X500, X1000 and X5000 were examined using Field Emission Scanning Electron Microscopy (FESEM) at accelerating voltage of 4.0 kV. Prior to scanning, the samples were placed on a disc and held in place using a double-sided carbon tape. The samples were then coated with platinum particles to avoid sample charging. The model of equipment used was JOEL JSM 6701F.

3.8.3 X-Ray Diffraction (XRD)

XRD analysis was carried out using Siemens XRD Diffractometer 5000 to understand the interlayer spacing of NBR/GO membranes using Nickel filtered Copper Kα radiation with $\lambda = 0.154$ nm. The samples were scanned with rate of 2°/min between 10-60°.

The interlayer spacing was calculated by Bragg's Equation in Equation 3.8:

$$d = \frac{n\lambda}{2sin\theta} \tag{3.8}$$

where

d = interlayer spacing (Armstrong)

λ = wavelength

3.9 Performance Test

3.9.1 Tensile Test

Tensile test was carried out according to American Society for Testing and Materials (ASTM) D638 standard under ambient condition to measure the elastic modulus, ultimate tensile strength and elongation at break of NBR and NBR/GO membranes. The specimens as displayed in Figure 3.6 were cut using dumbbell press cutter prior to testing. The test was conducted using Tinius Olsen H10KS-0748 light weight tensile tester as shown in Figure 3.7 with a load cell of 500 N, at a crosshead speed of 500 mm/min. The gage length, thickness and the diameter of the gage were measured. A total of 5 tensile test specimen were used for each loading of GO.

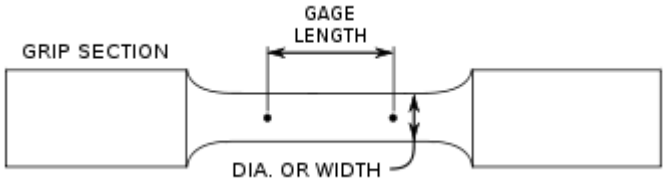

Figure 3.6: Specimen for Tensile Test.

Figure 3.7: Tinius Olsen H10KS-0748 Light Weight Tensile Tester.

3.9.2 Wastewater Preparation

Synthetic oily wastewater and also known as emulsified wastewater was prepared and used to investigate the performance of membrane samples. The wastewater was prepared using diesel oil, sodium dodecyl sulphate (SDS) and deionized water. The oil content in the synthetic wastewater was 1000 ppm which indicates 1g of diesel was mixed into 1L feed along with 0.01 wt% of SDS. The mixture was mildly heated and stirred for 30 minutes. No visible phase separation occurred using this mixing condition as shown in Figure 3.8.

The oil droplet size distributions in the wastewater were estimated with a particle counter (LIGHTHOUSE, LS-20) which can provide size readings in eight different size channels of 1.0, 2.0, 5.0, 7.0, 10.0, 15.0, 25.0 and 50.0 μm. It was found that the oil droplet sizes in the wastewater covered all channels from 1 to 50 μm but the majority was more normally distributed at the size around 7 μm.

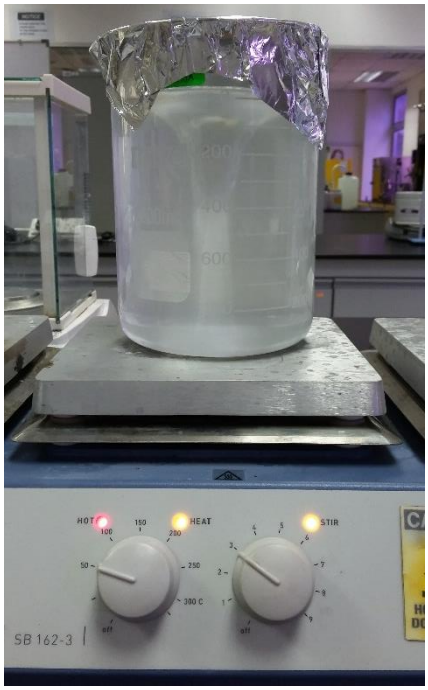

Figure 3.8: Preparation of Synthetic Oily Wastewater.

3.9.3 Permeation Flux Test for Synthetic Oily Wastewater

Performance of the membrane in terms of permeation flux and oil rejection rate was tested with pressure of 0.5 bar under room temperature. The test was conducted using a dead end membrane test rig (as shown in Figure 3.9) with a membrane effective surface area of 1.0179×10^{-3} m². Nitrogen gas was used as the pressure source. The filtrate was then collected for quantifying. The amount of filtrate to be collected was fixed to 30 ml.

Figure 3.9: Dead End Membrane Test Rig.

The permeation was calculated using Equation 3.9.

$$J_p = \frac{V_p}{A \times t} \tag{3.9}$$

where

J_p = Permeate Flux, $\frac{L}{m^2.hr}$

V_p = Permeate volume collected, L

A = Effective membrane area, m^2

t = Time taken to collect the measured amount of permeate, hr

3.9.4 Oil Rejection Rate Test for Synthetic Oily Wastewater

The Chemical Oxygen Demand (COD) and Total Oil Content (TOC) Analysis was used to determine the rejection rate of synthetic oily wastewater (Wang et al., 2012). COD value was obtained using Hach 2800 COD analyzer. Initially, the feed and collected filtrate about 2 ml each were injected into a COD reagent vial respectively. The reagent vial was then heated in a COD block digester at 150 °C for 2 hours. At the

end of 2 hours, the reagents were allowed to cool to room temperature. After that, the COD value was obtained using DR-6000 UV-vis Spectrometer.

Oil content of the filtrate were obtained using OCMA-310 Oil Content Analyzer. The oil content analyzer requires 20 minutes warm up prior to the testing. First, zero calibration and span calibration were performed. Next, 10 ml of extraction solvent (S-316) and 20 ml of filtrate was injected into the measuring cell. One drop of hydrochloric acid (HCL) was then added. The result was then displayed at the LCD once the extraction, cell fill and measurement processes were completed and followed by the draining process. The rejection rate was then determined using Equation 3.10.

$$R = \left(1 - \frac{C_p}{C_f}\right) \times 100\ \% \tag{3.10}$$

where

R = Rejection rate, %

C_p = Concentration in the permeate, mg/L

C_f = Concentration in the feed, mg/L

CHAPTER 4

RESULTS AND DISCUSSION

4.1 Characterization of Graphite Nanofibre (GNF) and Graphite Oxide

4.1.1 Fourier Transform Infrared Spectroscopy (FTIR)

FTIR was carried out to identify the types of chemical bonds and functional groups in GNF and graphite oxide. The absorption frequency regions for the relevant functional groups in GNF and graphite oxide were summarized in Table 4.1.

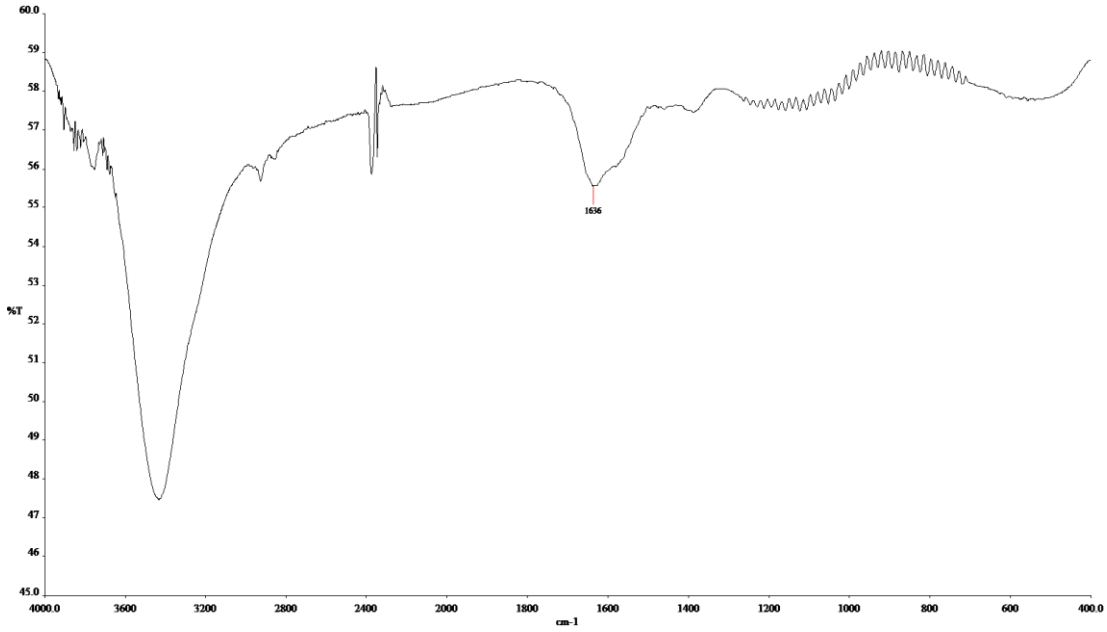

(a)

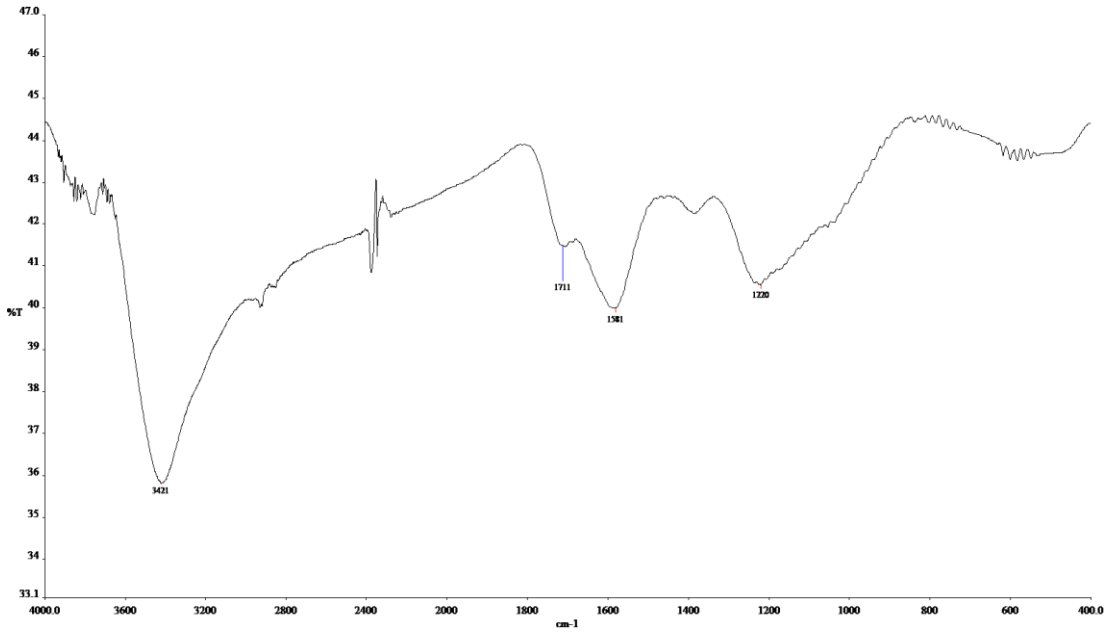

(b)

Figure 4.1: FTIR Spectra of (a) GNF and (b) Graphite Oxide.

Table 4.1: Absorption Frequency Regions and Functional Groups.

Absorption Frequency (cm^{-1})	Absorption Frequency (cm^{-1})		Functional Groups
	GNF	Graphite Oxide	
3550 – 3200		3421	Alcohol/Phenol O-H Stretch
1780 – 1710		1711	Carboxylic Acid C=O Stretch
1750 – 1680			Carbonyl C=O Stretch
1700 – 1500	1636	1581	Aromatic C=C Bending
1300 – 1000		1220	C-O-C Stretch
1260 – 1000			Alcohol C-O Stretch
1320 – 1210			Carboxylic Acid C-O Stretch
1300 – 1100			Carbonyl C-C Stretch

The peak at 1636 cm^{-1} represents the existence of C=C bonds in GNF (Chung, 2015). For graphite oxide, the very intense peak at 3421 cm^{-1} indicates the stretching vibration of O-H groups of alcohol or phenol (Chung, 2015; Tran et al, 2014). GNF also have this peak but not intense because GNF have surface bound water. Moreover, peak at 1711 cm^{-1} evidences the C=O stretching of carboxylic acid or carbonyl (Tran et al, 2014). Peak at 1581 cm^{-1} gives indication of the unoxidised C=C bonds presence in graphite oxide. In addition, another peak at 1220 cm^{-1} specifies the vibration of C-O-C epoxide functional groups (Tay, 2015).

The FTIR spectra of graphite oxide has revealed the successful oxidation of GNF using Hummer's method through incorporation of oxygen-containing groups into the structure of GNF.

4.2 Characterization of NBR and NBR/GO Membranes

4.2.1 Fourier Transform Infrared Spectroscopy (FTIR)

Based on the FTIR spectra of NBR in Figure 4.2, the peak at 3324 cm^{-1} indicates O-H stretching of alcohol or phenol. Peak at 3035 cm^{-1} corresponds to C-H stretching of alkene. C=O stretching appears at 1663 cm^{-1} while N-H bending is visible at 1593 cm^{-1} (Kawashima and Ogawa, 2005). Absorption at 1442 cm^{-1} is due to the presence of O-H bending of carboxylic acid. The peaks observed at 1092 cm^{-1}, 1012 cm^{-1} and 741 cm^{-1} represent C-N stretching of amine, C-O stretching of alcohol and C-H bending respectively (Kawashima and Ogawa, 2005).

Compared to the spectra of NBR, the spectra for NBR/2.0 wt% GO membranes in Figure 4.2 shows there was visible peak at 1648 cm^{-1} due to C=O stretching while peak at 1593 cm^{-1} corresponding to N-H bending shifted to 1594 cm^{-1}. This was due to the polar functional groups of C=O and N-H forming hydrogen bonding (Kurnig, Szczesniak and Scheiner, 1987) with GO which possess oxygen containing groups such as –OH, C-O-C and C=O. Peak at 1718 cm^{-1} which is attributed by C=O stretching of carboxylic acid or carbonyl and peak at 1271 cm^{-1} which represents the vibration of C-O-C epoxide functional groups, stretching vibration of C-O of carboxylic acid or C-C stretching of carbonyl in GO became more visible in the polymer membrane filled with GO. The other functional groups of GO including O-H stretching at 3421 cm^{-1} and C=C bending at 1581 cm^{-1} are not visible as individual peaks as they overlap with broad peaks given rise by NBR. The assignment of the functional groups is summarized in Table 4.2.

In Figure 4.3, the FTIR spectra of NBR/2.0 wt% GO membranes at different curing times showed not much difference. Thus, the FTIR spectra of NBR/2.0 wt% GO membranes at different curing times has demonstrated that the curing time did not change the functional groups of the membrane.

Table 4.2: Assignment of Functional Groups to Peaks in FTIR Spectra.

Absorption Frequency (cm^{-1})	Absorption Frequency (cm^{-1})		Functional Groups
	NBR	2.0 wt% GO	
3550 – 3200	3324	3313	Alcohol/Phenol O-H Stretch
3100 – 3010	3035	3035	Alkenyl C-H Stretch
1780 – 1710		1718	Carboxylic Acid C=O Stretch
1750 – 1680			Carbonyl C=O Stretch
1680 – 1630	1663	1663	C=O Stretch
		1648	
1640 – 1550	1593	1594	N-H Bending
1440 – 1400	1442	1448	Carboxylic Acid O-H Bending
1300 – 1000		1271	C-O-C Stretch
1320 – 1210			Carboxylic Acid C-O Stretch
1300 – 1100			Carbonyl C-C Stretch
1200 – 1025	1092	1087	C-N Stretch (alkyl)
1260 – 1000	1012	1015	Alcohol C-O Stretch
770 – 730	741	753	C-H Bending (mono & ortho)

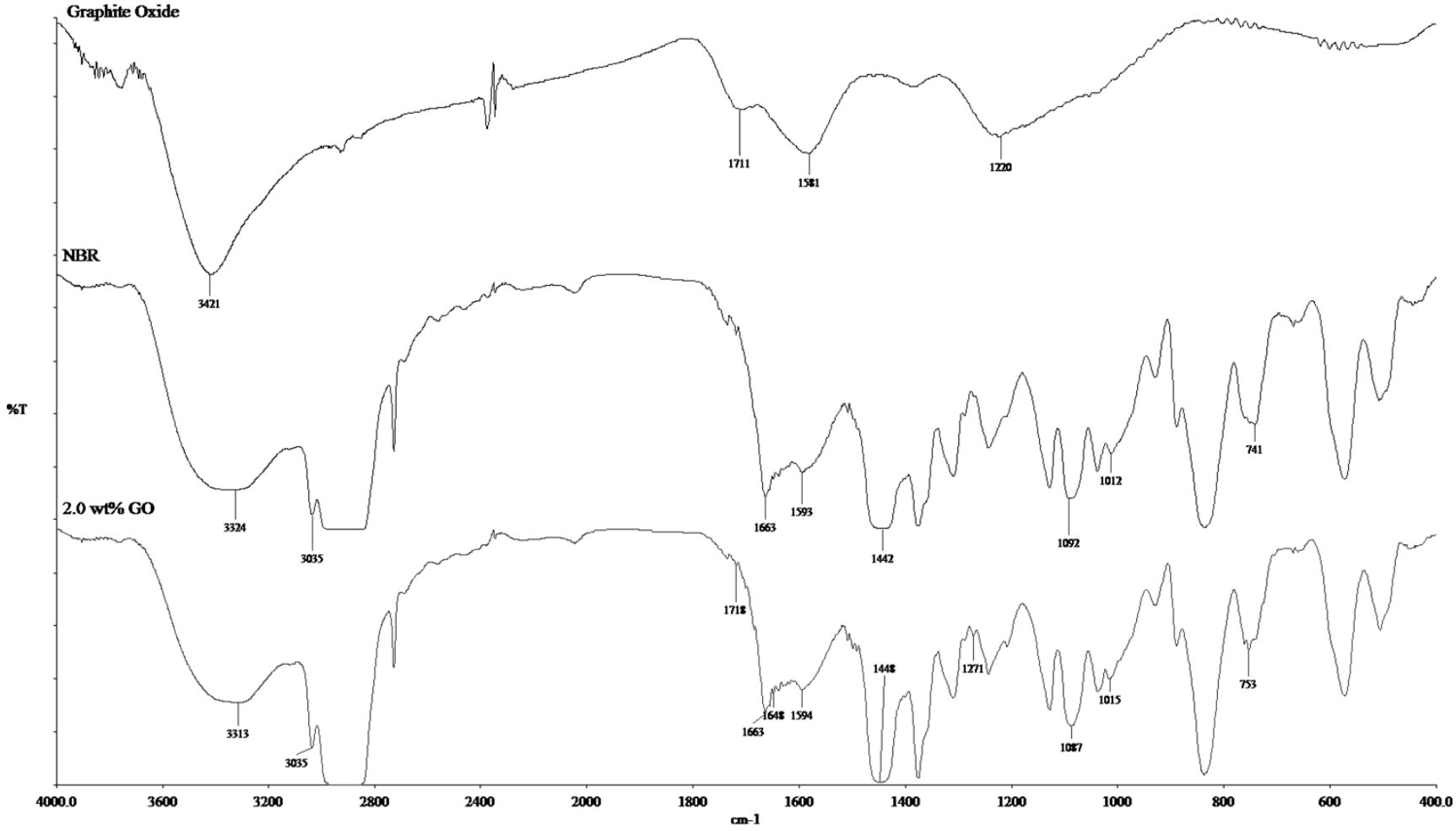

Figure 4.2: FTIR Spectra of Graphite Oxide, NBR and NBR/2.0 wt% GO Membranes.

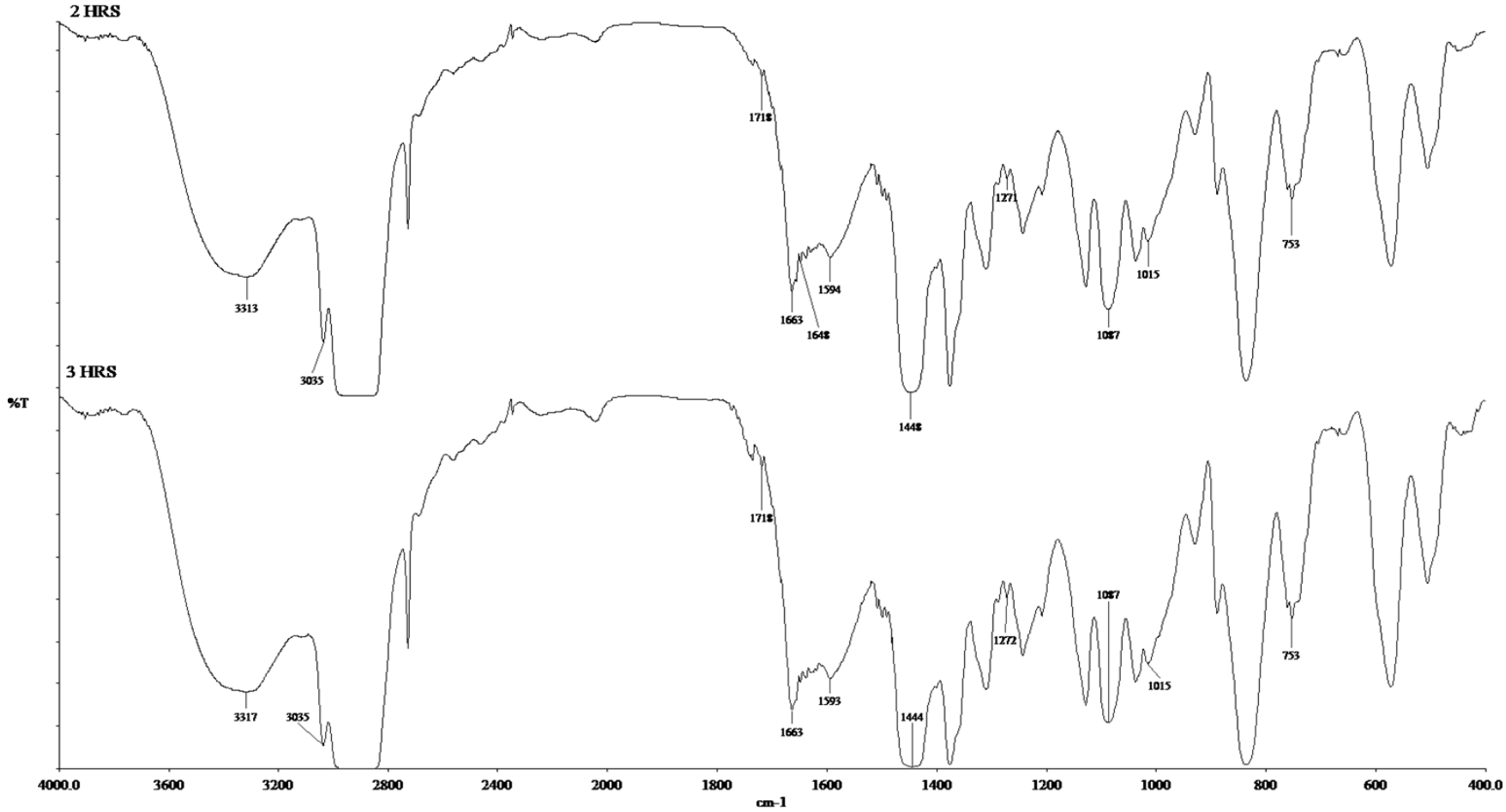

Figure 4.3: FTIR Spectra of NBR/2.0 wt% GO Membranes at Different Curing Times.

4.2.2 Field Emission Scanning Electron Microscopy (FESEM)

Morphology of NBR and NBR/GO was examined using FESEM. Figure 4.4 (a-b) shows the membrane surface of pure NBR membrane cured for 2 hours. At magnification of X200 and X5000, cracks on surface can be observed. In Figure 4.5 (a-b), the cracks on surface in NBR membrane cured for 3 hours were more severe compared to NBR membrane cured for 2 hours. This is due to the curing time effect on polymer matrix. The longer curing time caused higher cross-linking of the organic phase (Mohsen, Craig and Filisko, 1997). Hence, the membrane was over-cured caused increment in cracks on surface. Although there were cracks formation on the surface of the membranes, no water can pass through the membranes. Moreover, no pores could be observed at the surface of the both membranes.

Figure 4.6 (a-b) and Figure 4.7 (a-b) illustrate the images of NBR/0.5 wt% GO membranes cured for 2 hours and 3 hours respectively. The dark phases indicates the presence of GO sheets on the surface of the membranes. The low density of GO could promote the GO to travel to the surface of the latex membrane during curing process. GO filled in all the cracks on the membrane surface. Since GO covered all the cracks, it provides enhancement on the mechanical property of the membrane (Cui, Kundalwal and Kumar, 2016) but no pores can be noticed at the surface.

As compared to NBR/0.5 wt% GO, NBR/2.0 wt% GO exhibit much less cracks on surface as observed in Figure 4.8 (a-b) and Figure 4.9 (a-b). All the cracks were occupied by the GO as well. There was pores spotted at the surface of NBR/2.0 wt% GO cured for 2 hours in Figure 4.8 (a-b). The average pore size was 2.97 μm and can conclude that this membrane as microfiltration membrane since the average pore size fell in the range from 0.1 to 10 μm (Macedonio et al., 2012). On the other hand, no pores were detected at the surface of NBR/2.0 wt% GO cured for 3 hours because the membrane was over-cured. It formed very dense 3D network which might lead to no formation of pores. This caused the membrane had more wrinkles instead of having pores.

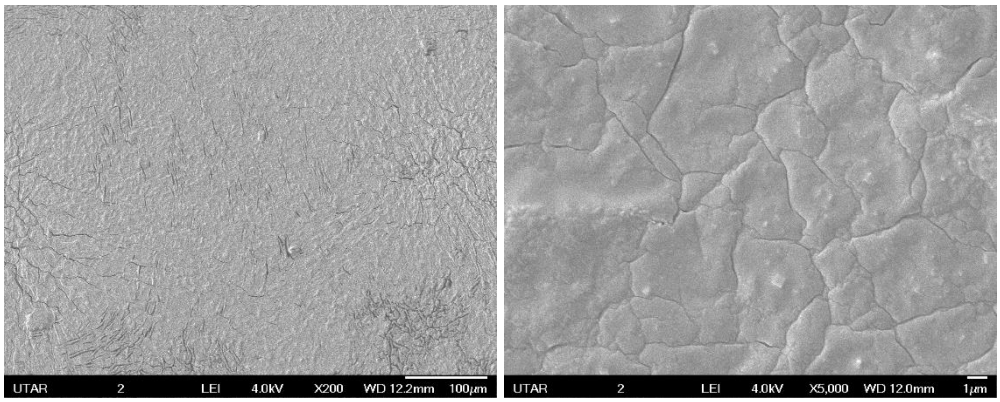

(a) (b)

Figure 4.4: SEM Images of NBR Membrane Cured for 2 Hours at Magnification of (a) X200 and (b) X5000.

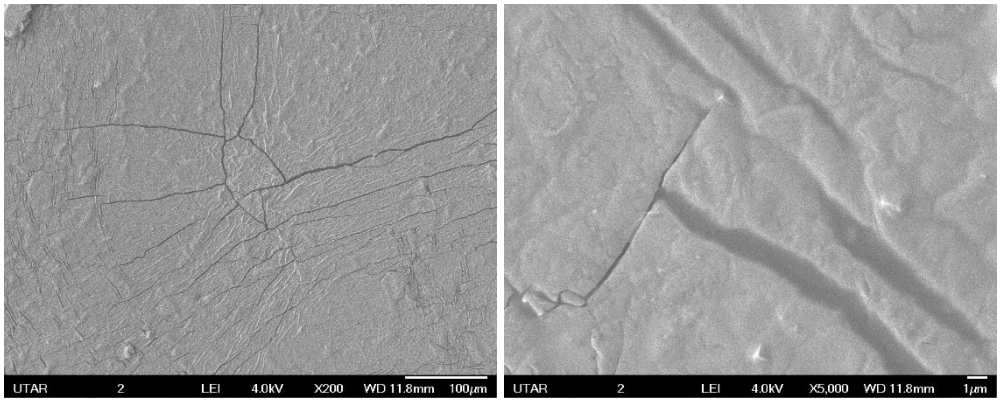

(a) (b)

Figure 4.5: SEM Images of NBR Membrane Cured for 3 Hours at Magnification of (a) X200 and (b) X5000.

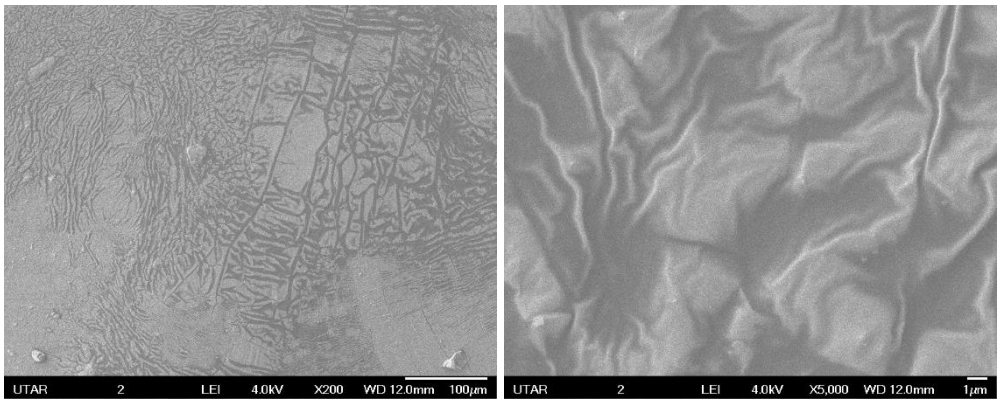

(a) (b)

Figure 4.6: SEM Images of NBR/0.5 wt% GO Membrane Cured for 2 Hours at Magnification of (a) X200 and (b) X5000.

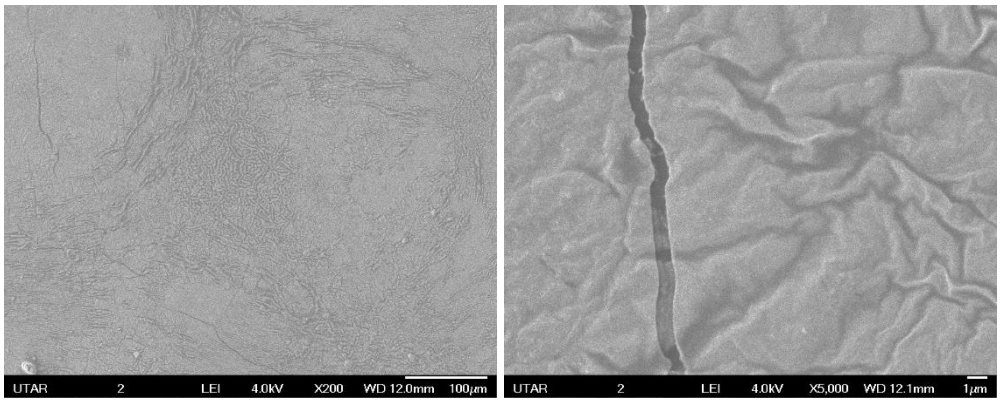

(a) (b)

Figure 4.7: SEM Images of NBR/0.5 wt% GO Membrane Cured for 3 Hours at Magnification of (a) X200 and (b) X5000.

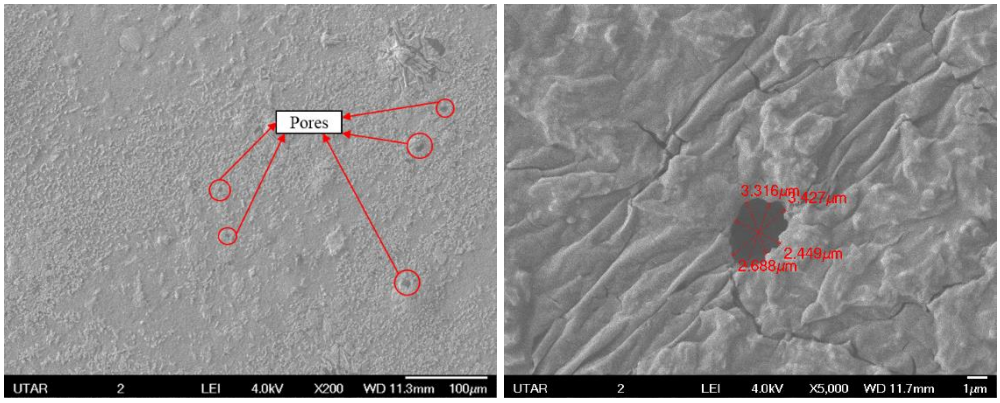

(a) (b)

Figure 4.8: SEM Images of NBR/2.0 wt% GO Membrane Cured for 2 Hours at Magnification of (a) X200 and (b) X5000.

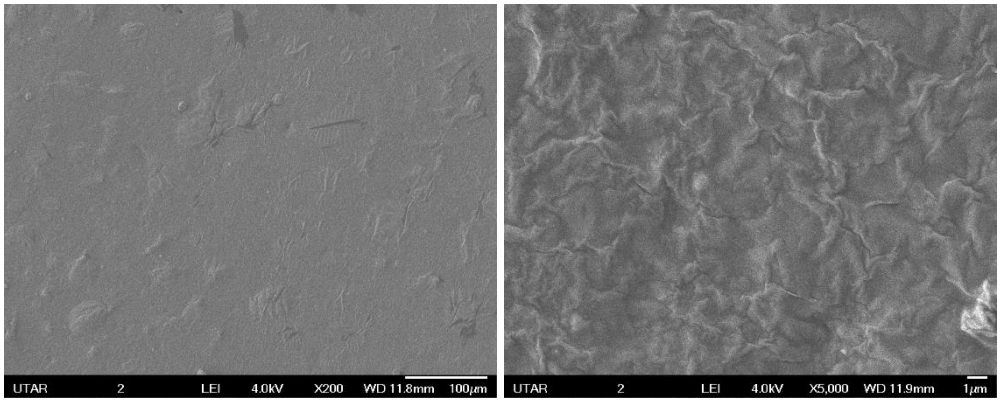

(a) (b)

Figure 4.9: SEM Images of NBR/2.0 wt% GO Membrane Cured for 3 Hours at Magnification of (a) X200 and (b) X5000.

4.2.3 X-Ray Diffraction (XRD)

The structure of NBR/GO membrane was also analysed using XRD. Figure 4.10 shows the XRD diffractogram for both GNF and graphite oxide. The XRD diffractogram for NBR/2.0 wt% GO at different curing times and NBR/GO with different loading of GO are illustrated by Figure 4.11 and 4.12.

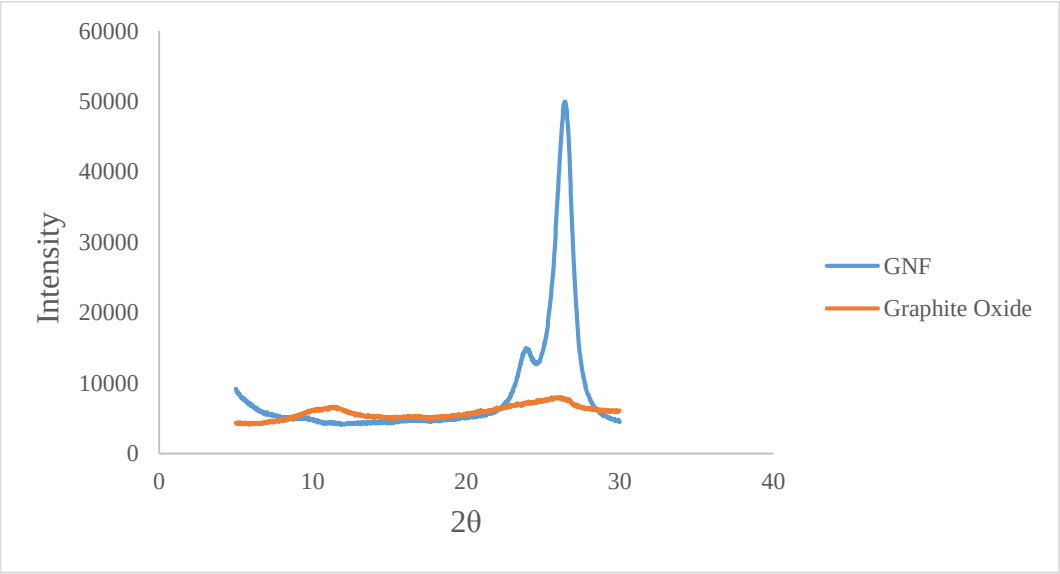

Figure 4.10: XRD Diffractogram of GNF and Graphite Oxide.

The diffraction peak of GNF that corresponds to the spacing between the graphitic layers around 0.3382 nm is at 2θ = 26.3281°. The graphite oxide produces a very low peak at the particular value, showing the conservation of some unoxidized graphitic surfaces (Chung, 2015). On the other hand, another peak appearing at around 12° corresponds to interlayer spacing of 0.7366 nm (Tay, 2015). This proved that the expansion in interlayer spacing because of the oxygen functionalities embedded in the layers (Ciszewski and Mianowski, 2013). In relation to this, Du, Qu and Zhang (2007) also reported a diffraction peak of graphite oxide at 2θ = 12.02°. The GNF has high intensity because it has more arranged structure compared to graphite oxide.

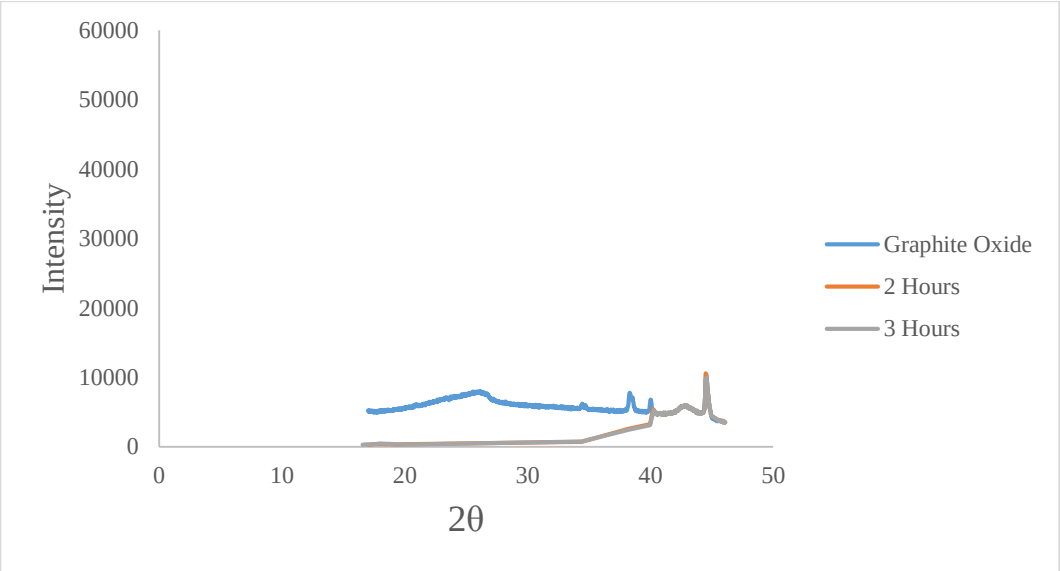

Figure 4.11: XRD diffractogram for NBR/2.0 wt% GO Membranes at Different Curing Times.

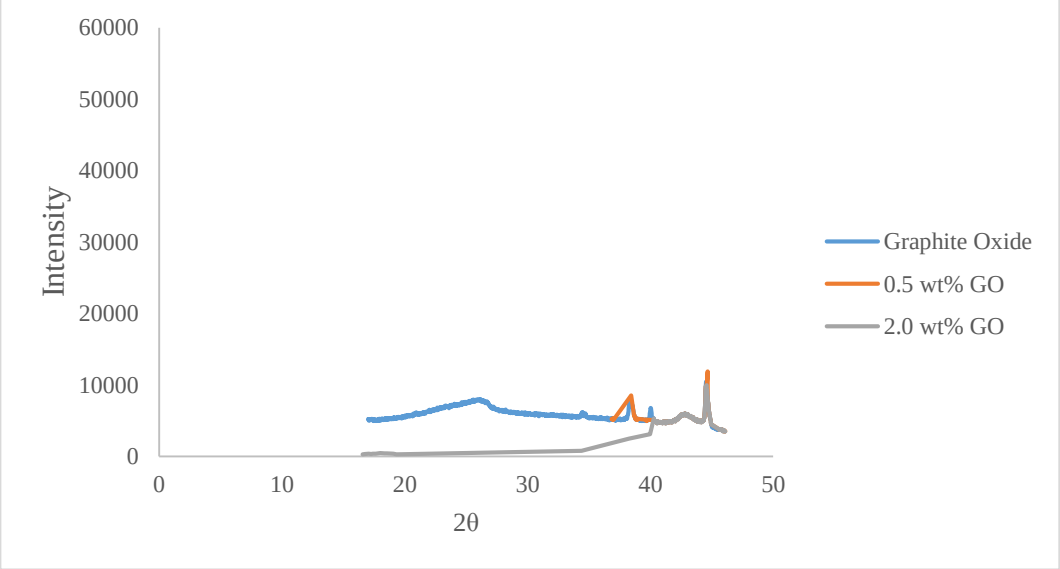

Figure 4.12: XRD Diffractogram for NBR/GO Membranes with Different Loading of GO.

According to the researches, no peak is observed for NBR in XRD due to its amorphous nature (Fabiula, Gerson and Carlos, 2011). The diffraction peak of NBR/2.0 wt% GO membrane at curing time of 2 hours at 2θ = 44.5024° corresponds to the spacing between the interlayer which is around 0.2034 nm. This showed the increment in interlayer spacing when the GO mixed in NBR matrix because the oxygen

functionalities embedded in the layers. The increment in interlayer spacing suggested the dispersion of GO in NBR matrix.

On the other hand, the diffraction peak at 2θ = 44.5031° corresponds to the spacing between the interlayer which is around 0.2034 nm as well for NBR/2.0 wt% GO which was cured for 3 hours. Both of the membranes indicate the same interlayer spacing. This findings demonstrated the curing time does not affect the dispersion of GO in NBR matrix.

Furthermore, compared to the NBR/2.0 wt% GO with NBR/0.5 wt% GO membranes, NBR membrane with 0.5 wt% loading of GO had diffraction peak at 2θ = 44.6714°. Moreover, it had an interlayer spacing of 0.2027 nm which indicated the decrement in interlayer spacing due to the graphene sheets were intercalated (Vilcinskas, 2017).

4.3 Performance Tests of NBR and NBR/GO Membranes

4.3.1 Tensile Test

Tensile test was carried out in order to study the mechanical properties of the NBR and NBR/GO membranes. Figure 4.13-4.15 illustrates the trend of the elastic modulus, ultimate tensile strength and elongation at break of NBR and NBR/GO membranes. The modulus, strength and elongation at break are summarized in Table 4.3.

Young's Modulus is ratio of the stress to the strain which measures the stiffness of a material. Tensile strength is the maximum stress that a material can bear before breaking while elongation at break known as fracture strain. The modulus, tensile strength and elongation at break showed a fluctuating trend with increasing percentage of GO in NBR. It can be observed from Figure 4.14 that the tensile strength of NBR/GO membranes cured for 2 hours are higher compared to pure NBR membrane. Addition of GO had clearly enhanced the tensile strength of the membrane (Zhang and Cho, 2017). GO is a well-known strong nanofiller with very high surface area for

interaction with polymer matrix (Papageorgiou, Kinloch and Young, 2015). A good-filler matrix interaction will promote stress transfer from matrix to filler and the nanocomposites will exhibit higher strength (Habib et al., 2017).

Moreover, the elongation at break of NBR/GO membranes cured for 2 hours are also higher compared to pure NBR membrane. From this observation, it can be said that the elasticity of the membrane had increased with the loading of GO (Papageorgiou, Kinloch and Young, 2015). On top of that, the NBR membrane with 0.5 wt% loading of GO showed the excellent mechanical property with higher elongation, tensile strength and break at elongation. This was due to the reinforcement effect of GO possessing very high stiffness, elasticity and strength (Thomas and Stephen, 2010). Strong interfacial interactions between GO and the NBR matrix also enabled the external load to be efficiently transferred through the interactions. Adding to that, the interaction of polymer chains with filler surfaces constrict the movement of the chains and may improve the modulus (Chow and Ishak, 2007). Furthermore, good dispersion of filler is also necessary for improvement in mechanical properties (Liu et al., 2003).

Based on the Figure 4.14, the error bars of NBR membrane with 1.0 wt%, 1.5 wt% and 2.0 wt% of GO loadings overlapped with error bar of pure NBR membrane which indicates there was no significant improvement with the increment of GO loadings. Hence, this resulted in fluctuating trend for NBR membrane with 1.0 wt%, 1.5 wt% and 2.0 wt% of GO loadings.

Figure 4.13-4.15 show that over-curing decrease the mechanical properties of membranes. Based on the findings from the tensile test, it can be concluded that the optimum curing time of NBR and NBR/GO membrane is 2 hours. Moreover, the addition of GO has proved to enhanced the overall performance and properties of the membrane.

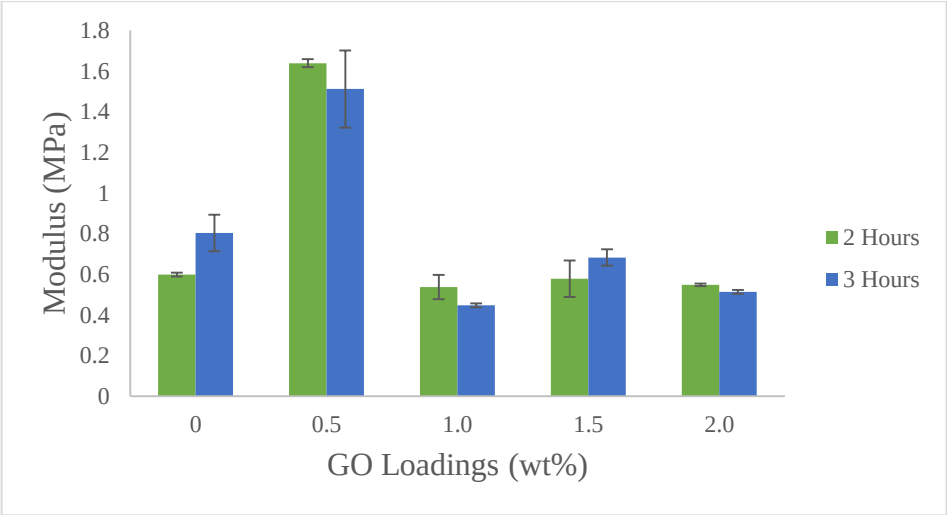

Figure 4.13: Young's Modulus of NBR and NBR/GO Membranes.

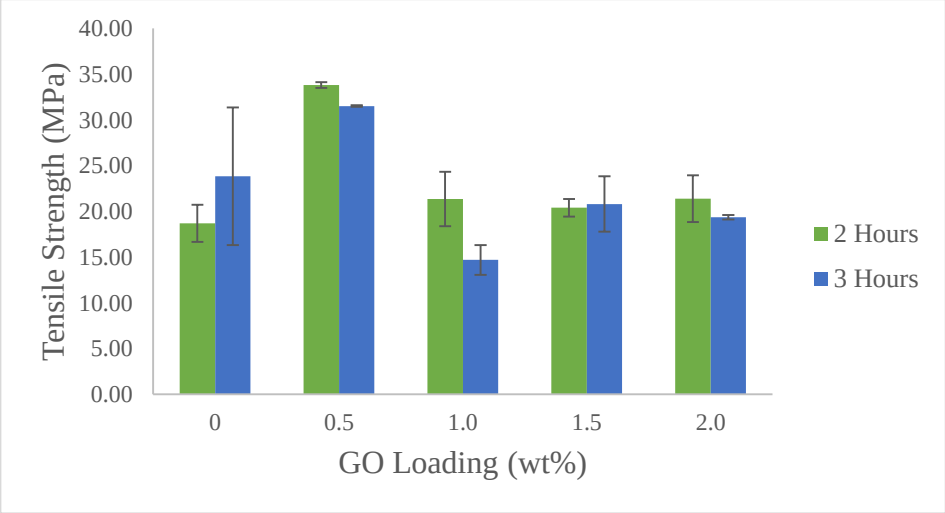

Figure 4.14: Tensile Strength of NBR and NBR/GO Membranes.

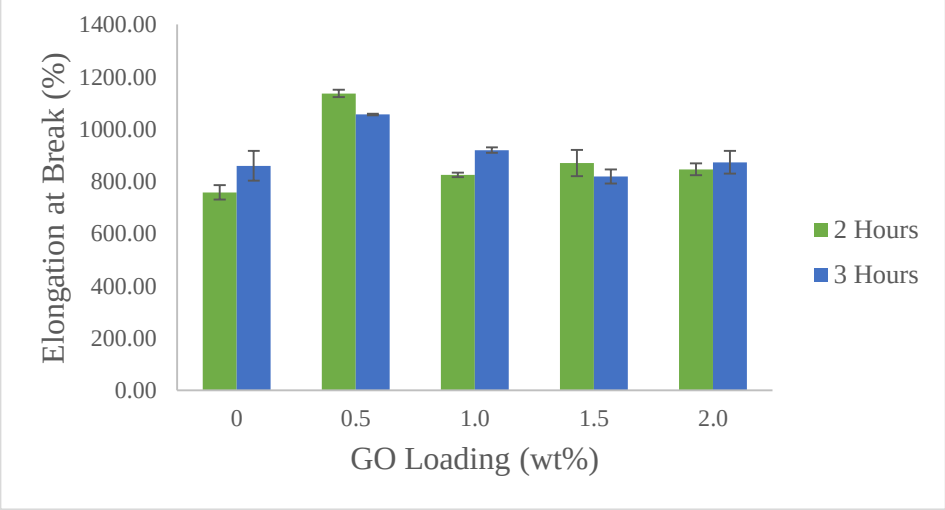

Figure 4.15: Elongation at Break of NBR and NBR/GO Membranes.

Table 4.3: Mechanical Properties of NBR and NBR/GO Membranes.

GO Loadings (wt%)	Young's Modulus (MPa)		Tensile Strength (MPa)		Elongation at Break (%)	
	2 hours	3 hours	2 hours	3 hours	2 hours	3 hours
0	0.599	0.804	18.70	23.84	757.50	859.50
0.5	1.639	1.512	33.82	31.52	1136.00	1056.00
1.0	0.537	0.448	21.35	14.70	825.00	919.50
1.5	0.578	0.683	20.40	20.81	870.25	819.00
2.0	0.549	0.514	21.39	19.37	846.00	873.00

4.3.2 Permeation Flux and Oil Rejection Rate Tests

NBR and NBR/GO membranes were tested using the dead end membrane filtration machine to study the performance of the membrane in terms of permeation flux and oil rejection rate. At higher pressure emulsified oil passes through the membranes (Sadrzadeh, Gorouhi and Mohammadi, 2008). Therefore, pressure must be lower than 1 bar for membrane filtration. Thus, the pressure was fixed at 0.5 bar. Another reason that 0.5 bar is preferred because from our previous study, the optimum rejection rate was obtained at this pressure. In addition, the filtrate of the test was also collected to quantify the oil content based on Chemical Oxygen Demand (COD) and Total Oil Content (TOC) analysis.

All the NBR and NBR/GO membranes except NBR/2.0 wt% GO membrane cured for 2 hours did not show any permeation flux, which means no water can go through the membranes. The reasons behind the zero permeation flux for pure NBR membranes are perhaps because of the chemical, water and oil resistance nature of the pure NBR film (Thomas, Marykutty and Mathew, 2013; Paran, Naderi and Ghoreishy, 2016) which did not promote selective permeability of water through the membrane. Membrane hydrophilicity plays and important factor in filtration which is associated with the surface adsorption properties of the membrane (Zhang et al., 2012). Thus, this early finding suggests that NBR alone could never be used as membrane material.

Based on the FESEM images, it was observed that only the membrane with 2.0 wt% GO loading cured for 2 hours has pores on membrane surface and allowed water to pass through with the permeation flux of 544.11$\left(\frac{L}{m^2.hr}\right)$. Moreover, addition of GO supplies oxygen functional group to the surface of the membrane, which contributes to the increased hydrophilicity of the NBR/GO membrane (Niyogi et al., 2006; Si and Samulski, 2008; Paredes et al., 2008). These factors had caused the hydrophilic water molecules to pass through the pores and increase the permeation flux. On the other hand, GO loadings of 0.5 wt%, 1.0 wt% and 1.5 wt% were not enough to increase the hydrophilicity of the membrane which resulted zero permeation flux.

Based on this data, it can be said that the optimum GO nanofiller loading and curing time for NBR/GO membrane are 2.0 wt% and 2 hours respectively. Regardless, the experiment data was able to prove that overall, addition of GO nanofillers clearly had made NBR a candidate for membrane production in oily wastewater filtration.

The result from permeation flux was further facilitated with the oil rejection rate test based on COD and TOC. The rejection rate was calculated using equation 3.9. The oil rejection rate based on TOC obtained is 85.5 % while the oil rejection rate based on COD is 58.6 %. It can be noticed that the rejection rate based on COD is lower compared to the rejection rate based on TOC because of the presence of surfactant inside the filtrate.

The oil rejection rate obtained is consider as low because emulsified oil can pass through the pores on membrane surface. The oil droplet size distributions in the wastewater were estimated with a particle counter (LIGHTHOUSE, LS-20) which can provide size readings in eight different size channels of 1.0, 2.0, 5.0, 7.0, 10.0, 15.0, 25.0 and 50.0 μm. It was found that the oil droplet sizes in the wastewater covered all channels from 1 to 50 μm. Thus, the oil droplet sizes which are less than the average pore size created on membrane surface (2.97 μm) able to pass through the pores. Therefore, the oil rejection rate was reduced. The values of permeation flux and rejection rate (COD and TOC) are summarized in Table 4.3.

Table 4.4: Water Flux and Oil Rejection Rate.

Membrane	Curing Time (hr)	Permeation Flux $\left(\frac{L}{m^2.hr}\right)$	Rejection Rate (COD) (%)	Rejection Rate (TOC) (%)
NBR/2.0 wt% GO	2	544.11	58.6	85.5

Overall the NBR/GO membrane can filter oil from oily wastewater. Additionally, GO nanosheets also have excellent intrinsic lubrication effect on the surface which will avoid the clogging of oil on the surface of the GO nanosheets (Kumar and Wani, 2017). The conducted test proves that NBR/GO has the mechanical strength to withstand the operating pressure of 0.5 bar. This implies that the membrane have potential not only for lab scale testing but can be commercialized and also utilized in industries.

CHAPTER 5

CONCLUSION AND RECOMMENDATIONS

5.1 Conclusion

NBR and NBR/GO membranes were successfully developed through latex compounding and curing method. The optimum curing time and GO formulation and its effect on NBR and NBR/GO membranes had been determined. Moreover, the NBR and NBR/GO membranes had also been characterized through FTIR, FESEM and XRD and the tensile properties of the membranes had been evaluated. Performance of the membranes in term of permeation flux and oil rejection rate had been analyzed.

The FTIR spectra proved the successful oxidation of GNF to graphite oxide using conventional Hummer's Method. In addition, characterization of NBR/GO membranes by FTIR indicated the interactions between GO and NBR through hydrogen bonding. Moreover, the effects of intercalation of graphene sheets on interlayer spacing were determined through XRD.

FESEM images shows that GO and pores could be observed at the surface of the NBR latex membrane. GO had occupied all the cracks on the surface of the membrane during the casting and curing process. Moreover, no pores were observed for pure NBR, NBR/0.5 wt% GO membranes cured for 2 and 3 hours and NBR/2.0 wt% GO cured for 3 hours at image magnification of X200 and X5000. Adding on this, pores were spotted on the surface of NBR membrane with 2.0 wt% GO loading cured for 2 hours.

The analysis on the mechanical properties of the NBR and NBR/GO membranes had proved that the overall properties of the membrane enhanced with the addition of GO and decreased with increment of curing time.

NBR and NBR/GO membranes were tested at pressure of 0.5 bar to investigate the flux behavior, using synthetic oily wastewater. Based on the results obtained, pure NBR membrane was unable to filter the oily wastewater as water permeation through the pure NBR membrane did not occur. This finding proved that NBR alone could never be used as membrane material. In contrast, only the NBR/2.0 wt% GO membrane cured for 2 hours was able to filter the oily wastewater. Addition of GO nanofiller had clearly made NBR a candidate to be produced as a membrane for oily wastewater filtration. The permeation flux that obtained was at $544.11\left(\frac{L}{m^2.hr}\right)$. The result from permeation flux was further facilitated with the oil rejection rate test based on COD and TOC. The oil rejection rate based on TOC obtained is 85.5 % while the oil rejection rate based on COD is 58.6 %. The results and data retrieved showed that NBR/GO membrane could reject oil. Thus, it can be concluded that the optimum curing time and GO formulation for NBR and NBR/GO membranes are 2 hours and 2.0 wt% respectively.

5.2 Recommendations

This study has demonstrated the performance of NBR and NBR/GO membranes through tensile properties, permeation flux and oil rejection rate. The potential of GO as promising filler in NBR has been proven. Based on the obtained result, GO is proven to be able to improve the performance and overall properties of NBR membrane. Some steps can be done in order to enhance the performance of the membrane. The following are some of the recommendations proposed in order to obtain the best possible performance from the nanocomposite membrane.

- Testing the NBR/GO membrane with different parameter of feed, namely, concentration of feed, temperature of feed.

- Vary the testing conditions in order to study the behaviour of NBR and NBR/GO membrane.

- Determine the dispersion pattern of GO in polymer matrix. The dispersion pattern may affect the properties of the nanocomposites produced. This can be done by Transmission Electron Microscopy (TEM).

- Prior exfoliation may further increase the surface-to-volume ratio of GO in the polymer matrix and bring greater improvement in the properties.

- Increase the sampling number for tensile test so that can reduce the standard deviation value.

REFERENCES

Almarzooqi, F. A., Ghaferi, A. A. A., Saadat, I. and Hilal, N. (2014). Application of Capacitive Deionisation in water desalination: A review. *Desalination (2014)*.

Al-Shamrani, A.A., Jamesa, A. and Xiao, H. (2002). *Colloids Surf.*, A209, pp.15-26.

Ammar, A., Al-Enizi, A.M., AlMaadeed, M.A., and Karim, A. (2015). Influence of graphene oxide on mechanical, morphological, barrier, and electrical properties of polymer membranes. *Arabian Journal of Chemistry*. [online] Available at: < https://www.researchgate.net/publication/282534266_Influence_of_Graphene_Oxide_on_Mechanical_Morphological_Barrier_and_Electrical_Properties_of_Polymer_Membranes> [Accessed 15 July 2017].

Asatekin, A. and Mayes, A.M. (2009). Oil Industry Wastewater Treatment with Fouling Resistant Membranes Contaning Amphiphilic Comb Copolymer. *Envrion. Sci. Technol.*, 43, pp.4487-4492.

Ashaghi, K.S., Ebrahimi, M. and Czermak, P. (2007).Ceramic ultra- and nanofiltration membranes for oilfield produced water treatment: a mini review. *Open Environ. J.* 1 (1), pp.1–8.

Belkacem, M., Matamoros, H., Cabassud, C., Aurelle, Y. and Cotteret, J. (1995). New results in metal working wastewater treatment using membrane technology. *J. Membr. Sci.*, 106, pp.195–205.

Brodie, B. (1859). On the Atomic Weight of Graphite. *Philosophical Transactions of the Royal Society of London*, 149, pp.249-259.

Bykkam, S., Rao, K.V., Chakra C.H.S. and Thunugunta, T. (2013). Synthesis and Characterization of Graphene Oxide and Its Antimicrobial Activity against Klebseilla and Staphylococus. *International Journal of advanced Biotechnology and Research*, 4(1), pp.142-146.

Chow, W. and Mohd Ishak, Z. (2007). Mechanical, morphological and rheological properties of polyamide 6/organo-montmorillonite nanocomposites. *expresspolymlett*, 1(2), pp.77-83.

Chung, C.S. (2015). *Development of Natural Rubber/Graphene Derivatives-Bentonite Nanocomposites.* BEng. Universiti Tunku Abdul Rahman.

Ciszewski, M. and Mianowski, A. (2013). *Survey of graphite oxidation methods using oxidizing mixtures in inorganic acids – Chemik International*. [online] Chemik International. Available at: http://www.chemikinternational.com/year-2013/year-2013-issue-4/survey-of-graphite-oxidation-methods-using-oxidizing-mixtures-in-inorganic-acids/ [Accessed 15 July 2017].

Cote, L., Kim, F. and Huang, J. (2009). Langmuir-Blodgett Assembly of Graphite Oxide Single Layers. *J. Am. Chem. Soc.*, 131(3), pp.1043-1049.

Cui, Y., Kundalwal, S. and Kumar, S. (2016). Gas barrier performance of graphene/polymer nanocomposites. *Carbon*, 98, pp.313-333.

Dickhout, J.M., Moreno, J., Biesheuvel, P.M., Boels, L., Lammertink, R.G.H. and de Vos, W.M. (2016). Produced water treatment by membranes: A review from a colloidal perspective. *Journal of Colloid and Interface Science*, 487(2017), pp.523-534.

Dreyer, D., Park, S., Bielawski, C. and Ruoff, R. (2009). The chemistry of graphene oxide. *Chem. Soc. Rev.*, 39(1), pp.228-240.

Du, L., Qu, B. and Zhang, M. (2007). Thermal properties and combustion characterization of nylon 6/MgAl-LDH nanocomposites via organic

modification and melt intercalation. *Polymer Degradation and Stability*, 92(3), pp.497-502.

Erickson, K., Erni, R., Lee, Z., Alem, N., Gannett, W. and Zettl, A. (2010). Determination of the Local Chemical Structure of Graphene Oxide and Reduced Graphene Oxide. *Adv. Mater.*, 22(40), pp.4467-4472.

Fabiula D.B. de Sousa, Gerson L.M. and Carlos H.S. (2011). Mechanical properties and morphology of NBR with different clays. *Polymer Testing*, 30(8), pp.819-825.

Fakhru'l-Razi, A., Alireza, P., Luqman Chuah, A., Dayang Radiah, A.B., Madaeni, S.S. and Zurina, Z.A. (2009). Review of technologies for oil and gas produced water treatment. *J. Hazard. Mater*., 170, pp.530–551.

Fu, X. and Qutubuddion, S. (2001). Polymer-clay nanocomposites: exfoliation of organophilic montmorillonite nanolayers in polystyrene. *Polymer*, 42(2), pp.807-813.

Ganesh, B., Isloor, A. M. and Ismail, A. (2013). Enhanced hydrophilicity and salt rejection study of graphene oxide-polysulfone mixed matrix membrane. *Desalination*, 313, pp.199-207.

Gao, W., Alemany, L., Ci, L. and Ajayan, P. (2009). New insights into the structure and reduction of graphite oxide. *Nature Chem*, 1(5), pp.403-408.

Gryta, M., Karakulski, K. and Morawski, A.W. (2001). Purification of oily wastewater by hybrid UF/MD. *Water Res*., 35, pp.3665–3669.

Habib, N., Chieng, B., Mazlan, N., Rashid, U., Yunus, R. and Rashid, S. (2017). Elastomeric Nanocomposite Based on Exfoliated Graphene Oxide and Its Characteristics without Vulcanization. *Journal of Nanomaterials*, 2017, pp.1-11.

Hanhi, K., Poikelispaa, M. and Tirila, H.M. (2007). *Elastomeric Materials*, Tampere University of Technology, The Laboratory of Plastics and Elastomer Technology.

Jamaly, S., Giwa, A. and Hasan, S.W. (2015). Recent improvements in oily wastewater treatment: Progress, challenges, and future opportunities. *Journal of Environmental Science*, 37(2015), pp.15-30.

Kawashima, T. and Ogawa, T. (2005). Prediction of the Lifetime of Nitrile-Butadiene Rubber by FT-IR. Analytical Sciences, 21, pp.1475-1478.

Khulbe, K.C., Feng, C. and Matsuura, T. (2010). The art of surface modification of synthetic polymeric membranes. *J. Appl. Polym. Sci.*, 115 (2).

Klaysom, C., Hermans, S., Gahlaut, A., Van Craenenbroeck, S. and Vankelecom, I.F. (2013). Polyamide/Polyacrylonitrile (PA/PAN) thin film composite osmosis membranes: Film optimization, characterization and performance evaluation. *Journal of Membrane Science*, 445, pp.25-33.

Kong, J. and Li, K. (1999). Oil removal from oil-in-water emulsions using PVDF membranes. *Sep. Purif. Technol*., 16, pp.83–93.

Kriipsalu, M., Marques, M., Nammari, D.R. and William, H. (2007). *J. Hazard. Mater.*, 148, pp.616-622.

Krishna, H. J. (1989). *Introduction to Desalination Technologies*. Available from World Wide Web: http://texaswater. Tamu.Edu. [Accessed 15 July 2017].

Ku, S., Lee, M. and Park, C. (2012). Carbon-Based Nanomaterials for Tissue Engineering. *Advanced Healthcare Materials*, 2(2), pp.244-260.

Kumar, P. and Wani, M. (2017). Tribological Characterisation of Graphene Oxide as Lubricant Additive on Hypereutectic Al-25Si/Steel Tribopair. *Tribology Transactions*, pp.0-0.

Kurnig, I.J., Szczesniak, M.M. and Scheiner, S. (1987). Vibrational Frequencies and Intensities of HBonded Systems. 1:1 and 1:2 Complexes of NH3 and PH3 with HFVibrational frequencies and intensities of H-bonded systems. 1:1 and 1:2 complexes of NH3 and PH3 with HF. *J. Chem. Phys.*, 87(2214).

Lalia, B.S., Kochkodan, V., Hashaikeh, R. and Hilal, N. (2013). A review on membrane fabrication: structure, properties and performance relationship. *Desalination*, 326, pp.77–95.

Lawler, J. (2016). Incorporation of Graphene-Related Carbon Nanosheets in Membrane Fabrication for Water Treatment: A Review. *Membranes*, 6(4), p.57.

Lee, J., Chae, H., Won, Y. J., Lee, K., Lee, C., Lee, H. H., Kim, I. and Lee, J. (2013). Graphene oxide nanoplatelets composite membrane with hydrophilic and antifouling properties for wastewater treatment. *Journal of Membrane Science*, 448, pp.223-230.

Li, J., Zeng, X., Ren, T. and van der Heide, E. (2014). The Preparation of Graphene Oxide and Its Derivatives and Their Application in Bio-Tribological Systems. *Lubricants*, 2(3), pp.137-161.

Lin, Z.S. and Wen, W. (2003). *Mar. Environ. Sci.*, 22, pp.15-19.

Liu, G.H., Ye, Z.F., Tong, K. and Zhang, Y.H. (2013). *Biochem. Eng. J.*, 72, pp.48-53.

Liu, P., Zhang, X., Jia, H., Yin, Q., Wang, J., Yin, B. and Xu, Z. (2017). High mechanical properties, thermal conductivity and solvent resistance in graphene oxide/styrene-butadiene rubber nanocomposites by engineering carboxylated acrylonitrile-butadiene rubber. *Composites Part B: Engineering*, 130, pp.257-266.

Liu, T., Ping Lim, K., Chauhari Tjiu, W., Pramoda, K. and Chen, Z. (2003). Preparation and characterization of nylon 11/organoclay nanocomposites. *Polymer*, 44(12), pp.3529-3535.

Macedonio, F., Drioli, E., Gusev, A., Bardow, A., Semiat, R. and Kurihara, M. (2012). Efficient technologies for worldwide clean water supply. *Chemical Engineering and Processing: Process Intensification*, 51, pp.2-17.

Mackey, D. and Jorgensen, A.H. (1999). Elastomers, Synthetic (Nitrile Rubber). *Kirk-Othmer Concise Encyclopedia of Chemical Technology*, 4, pp.687-688.

Maguire-Boyle, S.J. and Barron, A.R. (2011). A new functionalizing strategy for oil/water separation membranes. *J. Membr. Sci*., 382, pp.107–115.

Marcano, D. C., Kosynkin, D. V., Berlin, J. M., Sinitskii, A., Sun, Z., Slesarev, A., Alemany, L. B., Lu, W. and Tour, J. M. (2010). Improved synthesis of graphene oxide. *ACS nano*, 4 (8), pp.4806-4814.

Matilainen, A., Liikanen, R., Nyström, M., Llndqvist, N. and Tuhkanen, T. (2004). Enhancement of the natural organic matter removal from drinking water by nanofiltration. *Journal Environmental Technology*, 25(3), pp.283-291.

Mensah, B., Kim, S., Arepalli, S. and Nah, C. (2014). A study of graphene oxide-reinforced rubber nanocomposite. *Journal of Applied Polymer Science*, 131(16).

Mittal, V. (2013). *Thermoset nanocomposites*. 1st ed. Weinheim, Germany: Wiley-VCH Verlag.

Mohsen, N.M., Craig, R.G. and Filisko, F.E. (1997). Effects of curing time and filler concentration on curing and postcuring of urethane dimethacrylate composites: A microcalorimetric study. pp.224-232.

Mondal, S. (2015). Polymer Nano-Composite Membranes. *Journal of Membrane Science & Technology*, 05(01).

Morillo, J., Usero, J., Rosado, D., El Bakouri, H., Riaza, A. and Bernaola, F. (2014). Comparative study of brine management technologies for desalination plants. *Desalination*, 336, pp.32-49.

Nitrile Rubber - NBR Rubber - ACME Rubber. (2017). *Nitrile- Rubber NBR Rubber –ACME Rubber*. [online] Available at: http://www.acmerubber.com/nitrile.htm [Accessed 15 July 2017].

Niyogi, S., Bekyarova, E., Itkis, M., McWilliams, J., Hamon, M. and Haddon, R. (2006).Solution Properties of Graphite and Graphene. *J. Am. Chem. Soc.*, 128(24), pp.7720-7721.

Padaki, M., Surya Murali, R., Abdullah, M.S., Misdan, N., Moslehyani, A., Kassim, M.A., Hilal, N. and Ismail, A.F. (2014). Membrane technology enhancement in oil-water separation. A review. *Desalination*, 357(2015), pp.197-207.

Papageorgiou, D., Kinloch, I. and Young, R. (2015). Graphene/elastomer nanocomposites. *Carbon*, 95, pp.460-484.

Paran, S., Naderi, G. and Ghoreishy, M. (2016). Mechanical properties development of high-ACN nitrile-butadiene rubber/organoclay nanocomposites. *Plastics, Rubber and Composites*, 45(9), pp.389-397.

Paredes, J. I., Villar-Rodil, S., Martinez-Alonso, A. and Tascon, J. M. D. (2008). *Langmuir*, 24, pp.10560–10564.

Paredes, J., Villar-Rodil, S., Martinez-Alonso, A. and Tascon, J. (2008). Grapheme Oxide Dispertions in Organic Solvents. Langmuir, 24(19), pp.10560-10564.

Park, S and Ruoff, R. (2009). Chemical methods for the production of graphenes. *Nature Nanotech*, 4(4), pp.217-224.

Paul, D. and Robeson, L. (2008). Polymer nanotechnology: Nanocomposites. *Polymer*, 49(15), pp.3187-3204.

Pendergast, M.T.M. and Hock, E.M.V. (2011). A Review of Water Treatment Membrane Nanotechnologies. *Energy & Environmental Science.*, 4, pp.1946-1971.

Peng, X., Jin, J., Nakamura, Y., Ohno, T. and Ichinose, I. (2009). Ultrafast permeation of water through protein-based membranes. *Nature Nanotechnology*, 4, pp.353–357.

Phao, N., Nxumalo, E. N., Mamba, B. B. and Mhlanga, S. D. (2013). A nitrogen-doped carbon nanotube enhanced polyethersulfone membrane system for water treatment. *Physics and Chemistry of the Earth, Parts A/B/C*, 66, pp.148-156.

Potts, J., Dreyer, D., Bielawski, C. and Ruoff, R. (2011). Grapheme-based polymer nanocomposites. *Polymer*, 52(1), pp.5-25.

Qu, X., Alvarez, P. J. and Li, Q. (2013). Applications of nanotechnology in water and wastewater treatment. *Water research*, 47(12), pp.3931-3946.

Raidongia, K., Tan, A. and Huang, J. (2014). Graphene Oxide: Some New Insights into an Old Material. *Carbon Nanotubes and Graphene*, pp.341-374.

Ramanathan, T., Abdala, A., Stankovich, S., Dikin, D., Herrera-Alonso, M., Piner, R., Adamson, D., Schniepp, H., Chen, X., Ruoff, R., Nguyen, S., Aksay, I., Prud'Homme, R. and Brinson, L. (2008). Functionalized graphene sheets for polymer nanocomposites. *Nature Nanotech*, 3(6), pp.327-331.

Raza, H. (2012). *Graphene nanoelectronics*. Berlin: Springer, p.437.

Roads & Bridges. (2017). *How to Remove Emulsified Oil from Wastewater with Organoclays*. [online] Available at: https://www.roadsbridges.com/how-remove-emulsified-oil-wastewater-organoclays [Accessed 15 July 2017].

Sadrzadeh, M., Gorouhi, E. and Mohammadi, T. (2008). Oily Wastewater Treatment Using Polytetrafluoroethylene (PTFE) Hydrophobic Membranes. In: *Twelfth International Water Technology Conference*, IWTC12 2008 Alexandria, Egypt.

Salahi, A., Noshadi, I., Badrnezhad, R., Kanjilal, B. and Mohammadi, T. (2013). Nano-porous membrane process for oily wastewater treatment: Optimization using response surface methodology. *Journal of Environmental Chemical Engineering*, 1(3), pp.218-225.

Sarvini, B. (2017). *NBR Latex / Graphene Oxide Membrane for Wastewater Filtration*. BEng. Universiti Tunku Abdul Rahman.

Sean, G., Cheer, N. and Ismail, A. (2015). Current Progress of Nanomaterial/Polymer Mixed-Matrix Membrane for Desalination. *Membrane Fabrication*, pp.489-510.

Sengupta, R., Bhattacharya, M., Bandyopadhyayb, S. and Bhowmick, A. (2011). A review on the mechanical and electrical properties of graphite and modified graphite reinforced polymer composites. *Pro. Polym. Sci.*, 36(5), pp.638-670.

Shao, G., Lu, Y., Wu, F., Yang, C., Zeng, F. and Wu, Q. (2012). Graphene oxide: the mechanisms of oxidation and exfoliation. *Journal of Materials Science*, 47 (10), pp.4400-4409.

Si, Y. and Samulski, E. (2008).Synthesis of Water Soluble Graphene. *Nano Letters*, 8(6), pp.1679-1682.

Sirianuntapiboon, S. and Ungkaprasatcha, O. (2007). *Bioresour. Technol.*, 98, pp.2749-2757.

Song, L. F. (1998). Flux decline in crossflow microfiltration and ultrafiltration: mechanisms and modeling of membrane fouling. *J. Membr. Sci*., 139, pp.183–200.

Staudenmaier, L. (1898). *Ber. Dtsch. Chem. Ges.*, 31, pp.1481–1487.

Sun, A. C., Kosar, W., Zhang, Y. and Feng, X. (2014). Vacuum membrane distillation for desalination of water using hollow fiber membranes. *Journal of Membrane Science,* 455, pp.131-142.

Synderfiltration.com. (2017). *Membrane Materials: Organic v. Inorganic*. [online] Available at: http://synderfiltration.com/learning-center/articles/introduction-to- membranes/membrane-materials-organic-inorganic/ [Accessed 25 July 2017].

Tang, S.F. and Liu, F. (2006). *J. Oil Gas Technol.*, 28, pp.131-133.

Tay, Y.H. (2015). *Development of Nylon-6/Graphene Oxide (GO) High Performance Nanocomposites*. BEng. Universiti Tunku Abdul Rahman.

Thomas, S. and Stephen, R. (2010). *Rubber Nanocomposites*. 1st ed. Singapore: Wiley.

Thomas, S., Marykutty, C. and Mathew, E. (2013). Evaluation of Effect of Various Nanofillers on Technological Properties of NBR/NR Blend Vulcanized Using BIAT-CBS System. *Journal of Polymers*, pp.1-10.

Thostenson, E., Li, C. and Chou, T. (2005). Nanocomposites in context. *Composites Science and Technology*, 65(3-4), pp.491-516.

Tran, M., Yang, C., Yang, S., Kim, I. and Jeong, H. (2014). Influence of graphite size on the synthesis and reduction of graphite oxides. *Current Applied Physics*, 14, pp.S74-S79.

Vilcinskas, K., Mulder, F.M., Picken, S.J and Koper, G.J.M. (2017). In situ X-ray diffraction studies of graphite oxidation reaction indicating different exfoliation mechanism than ex site studies. Department of Chemical Engineering, Delft University of Technology, *van der Maasweg 9*.

Wang, M., Yan, C. and Ma, L. (2012). Graphene Nanocomposites. Composites and Their Properties. [online] Available at: http://www.intechopen.com/books/composites-and-their-properties/graphene-nanocomposites [Accessed 15 July 2017].

Wang, T. (2007). *Oil-Gasfield Surf. Eng.*, 26, pp.26–27.

Wang, Y., Ou, R., Ge, Q., Wang, H. and Xu, T. (2013). Preparation of polyethersulfone/carbon nanotube substrate for high-performance forward osmosis membrane. *Desalination*, 330, pp.70-78.

Wang, Z., Yu, H., Xia, J., Zhang, F., Li, F., Xia, Y. and Li, Y. (2012). Novel GO-blended PVDF ultrafiltration membranes. *Desalination*, 299, pp.50-54.

Wenyu, L., Linlin, Z. and Luhua, S. (2013). Biological Treatment Technology of Oily Sludge. *International Journal of Engineering Research and Development*, 8(3), pp.52-55.

Wilkinson, J. (2017). *Developing Graphene Oxide Membranes for the Purification of Water and Green Fuels*.

Wu, L., Ge, G. and Wan, J.B. (2009). *J. Environ. Sci.*, 21, pp.237-242.

Wu, T. and Ting, J. (2013). Preparation and characteristics of graphene oxide and its thin films. *Surface and Coatings Technology*, 231, pp.487-491.

Yan, L., Hong, S., Li, M. and Li, Y. (2009). Application of the Al_2O_3--PVDF nanocomposite tubular ultrafiltration (UF) membrane for oily wastewater treatment and its antifouling research. *Separation and Purification Technology*, 66(2), pp.347-352.

Yang, H., Shan, C., Li, F., Zhang, Q., Han, D. and Niu, L. (2009). Convenient preparation of tunably loaded chemically converted graphene oxide/epoxy resin nanocomposites from graphene oxide sheets through two-phase extraction. *Journal of Materials Chemistry*, 19(46), p.8856.

Yang, L., Thongsukmak, A., Sirkar, K.K., Gross, K.B. and Mordukhovich, G., (2011). Bio-inspired onboard membrane separation of water from engine oil. *J. Membr. Sci.*, 378, pp.138–148.

Yi, X., Yu, S., Shi, W., Sun, N., Jin, L., Wang, S., Zhang, B., Ma, C. and Sun, L. (2011). The influence of important factors on ultrafiltration of oil/water emulsion using PVDF membrane modified by nano-sized TiO2/Al2O3. *Desalination*, 281, pp.179-184.

Yu, L., Han, M. and He, F. (2013). A review of treating oily wastewater. *Arabian Journal of Chemistry*, 10(2017), pp.S1913–S1922.

Zavastin, D., Cretescu, I., Bezdadea, M., Bourceanu, M., Drăgan, M., Lisa, G., Mangalagiu, I., Vasiü, V. and Saviü, J. (2010). Preparation, characterization and applicability of cellulose acetate-polyurethane blend membrane in separation techniques. *Colloids Surfaces., A*, 370, pp.120–128.

Zeng, Y.B., Yang, C.Z., Zhang, J.D. and Pu, W.H. (2007). *J. Hazard. Mater.*, 147, pp.991-996.

Zhang, L., Chen, G., Tang, H., Cheng, Q. and Wang, S. (2009). Preparation and characterization of composite membranes of polysulfone and microcrystalline cellulose. *Journal of Applied Polymer Science*, 112(1), pp.550-556.

Zhang, S., Wang, R., Zhang, S., Li, G. and Zhang, Y. (2014). Treatment of wastewater containing oil using phosphorylated silica nanotubes (PSNTs)/polyvinylidene fluoride (PVDF) composite membrane. *Desalination*, 332(1), pp.109-116.

Zhang, X., Fan, X., Li, H. and Yan, C. (2012). Facile preparation route for graphene oxide reinforced polyamide 6 composites via in situ anionic ring-opening polymerization. *Journal of Materials Chemistry*, 22(45), pp.24081.

Zhang, Y. and Cho, U. (2017). Enhanced thermo-physical properties of nitrile-butadiene rubber nanocomposites filled with simultaneously reduced and functionalized graphene oxide. *Polymer Composites*.

Zhu, D.H. and Zheng, Z.H. (2002). *Environ. Prot. Petrochem. Ind.*, 25, pp.16-18.

Zhu, Y., Murali, S., Cai, W., Li, X. Suk, J., Potts, J. and Ruoff, R. (2010). Grapheme and Graphene Oxide: Synthesis, Properties and Applications. *Adv. Mater.*, 22(35), pp.3906-3924.

Zhu, Y., Murali, S., Stroller, M., Velamakanni, A, Piner, R. and Ruoff, R. (2010). Microwave assisted exfoliation and reduction of graphite oxide for ultracapacitors. *Carbon*, 48(7), pp.2118-2122.

Zhu, Y., Wang, D., Jiang, L. and Jin, J. (2014). Recent progress in developing advanced membranes for emulsified oil/water separation. *NPG Asia Materials*, pp.1-11.

APPENDICES

APPENDIX A: Fourier Transform Infrared Spectroscopy (FTIR)

(a) NBR Cured for 2 Hours

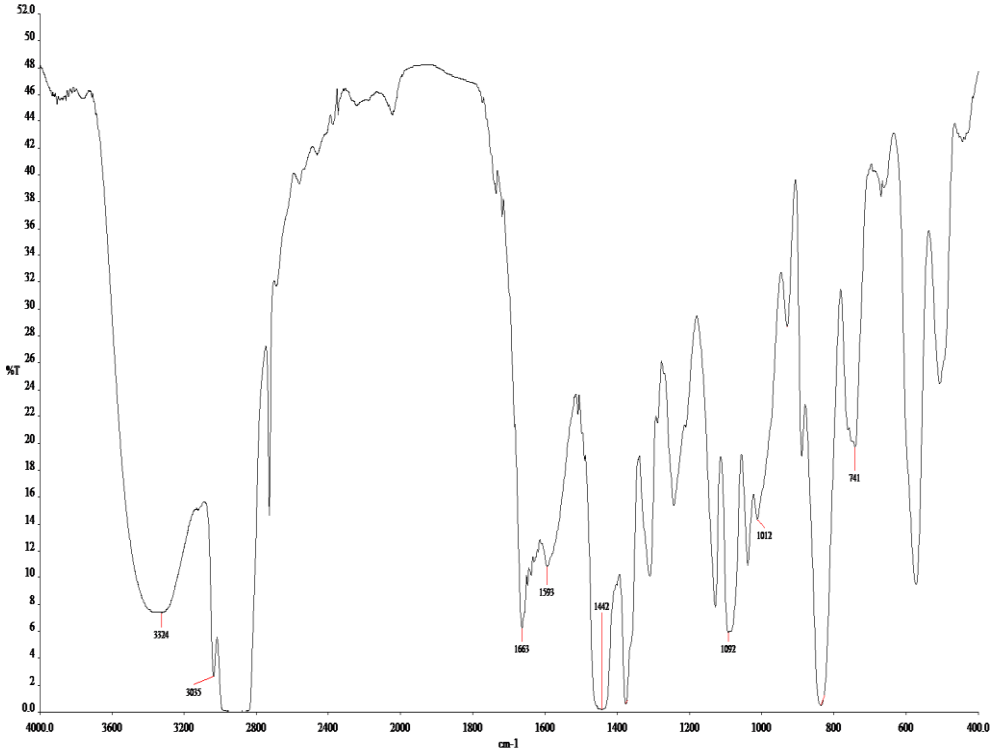

(b) NBR Cured for 3 Hours

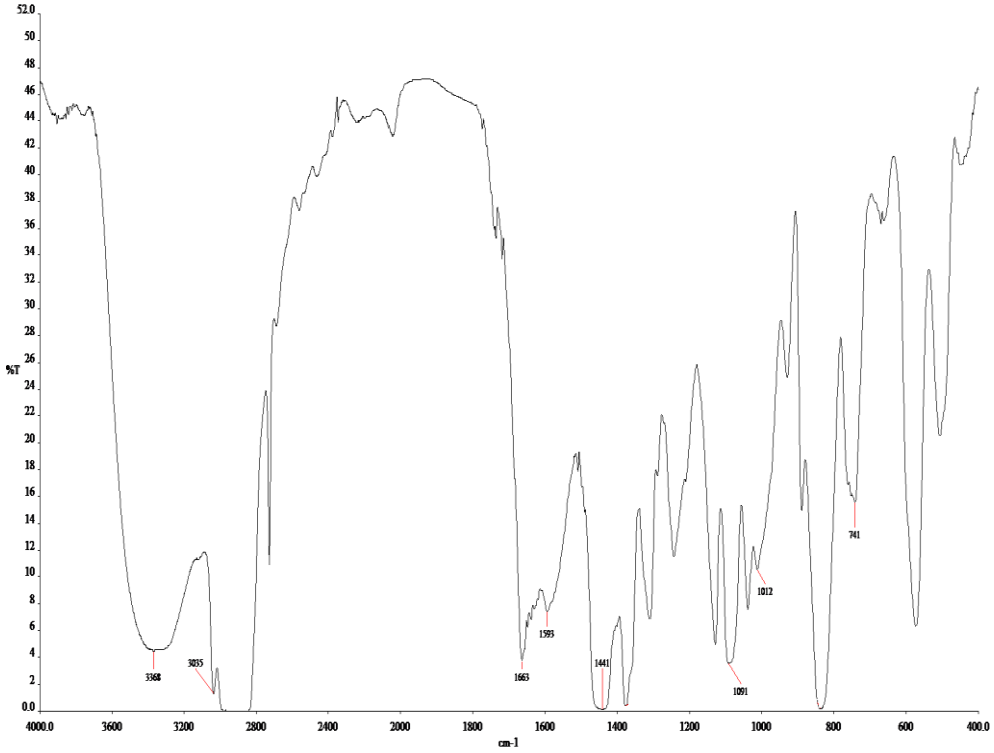

(c) NBR/0.5 wt% GO Cured for 2 Hours

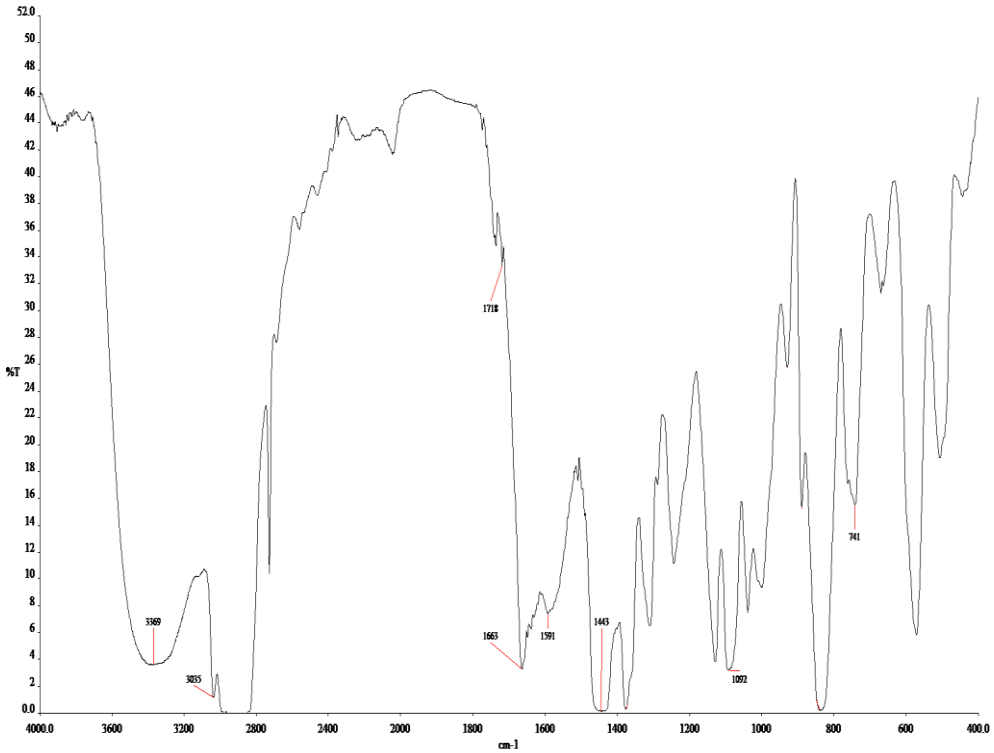

(d) NBR/0.5 wt% GO Cured for 3 Hours

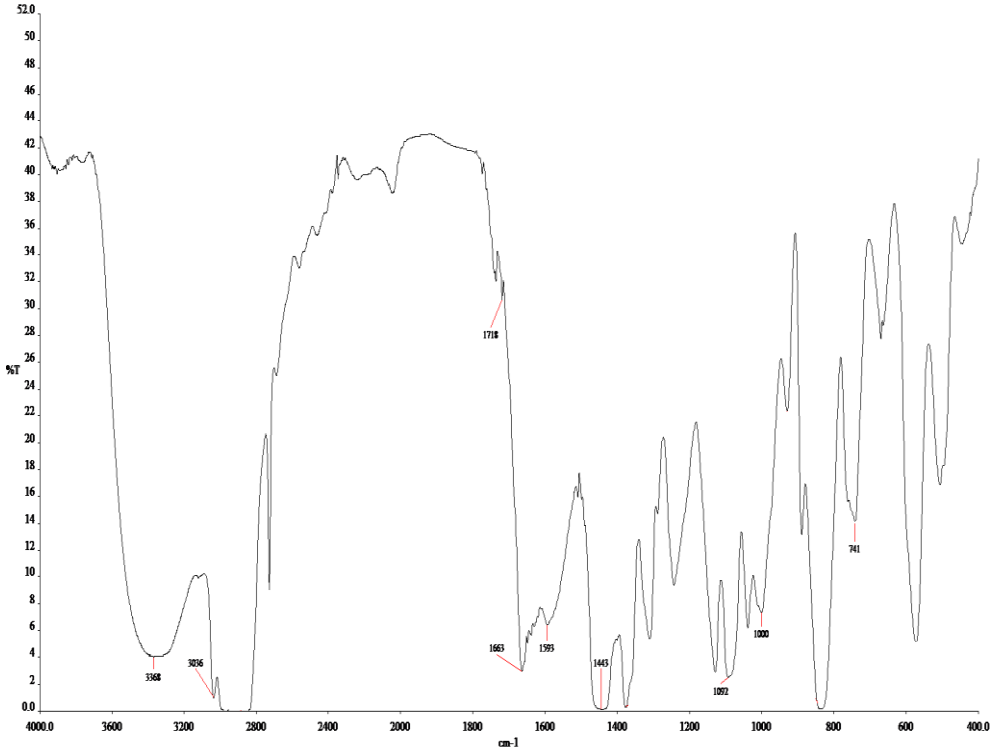

(e) NBR/1.0 wt% GO Cured for 2 Hours

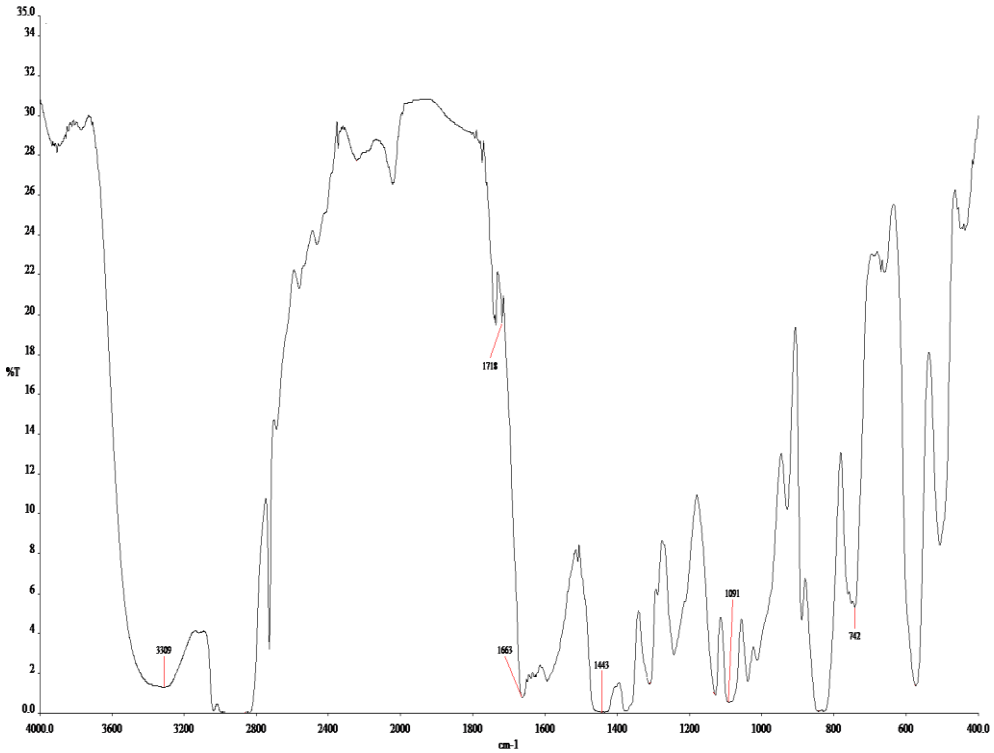

(f) NBR/1.0 wt% GO Cured for 3 Hours

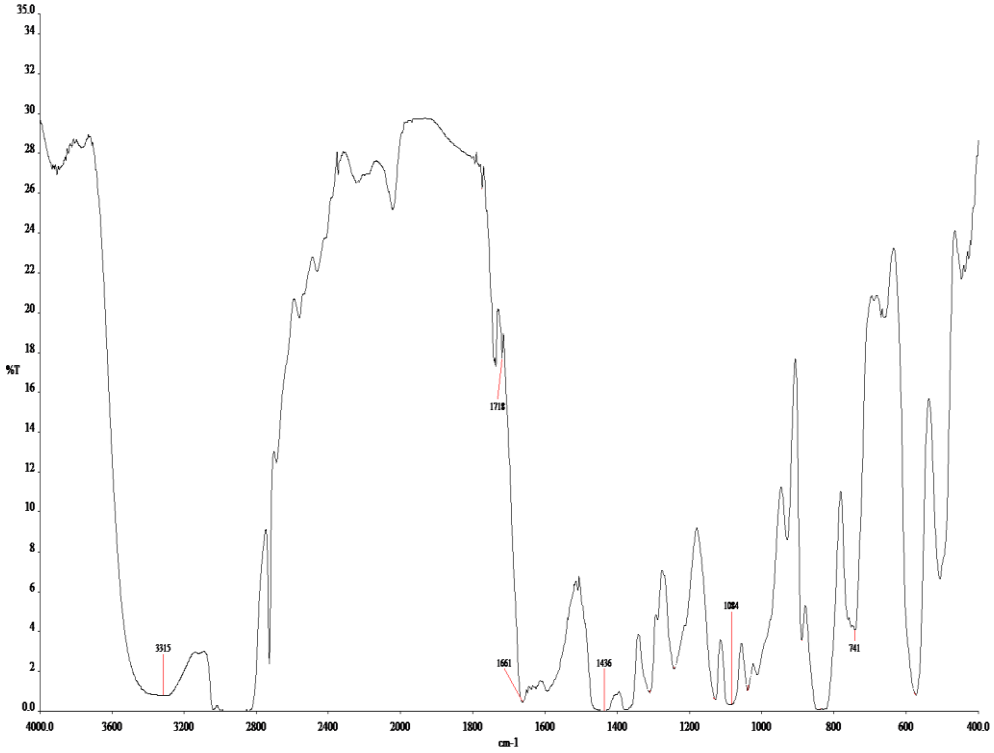

(g) NBR/1.5 wt% GO Cured for 2 Hours

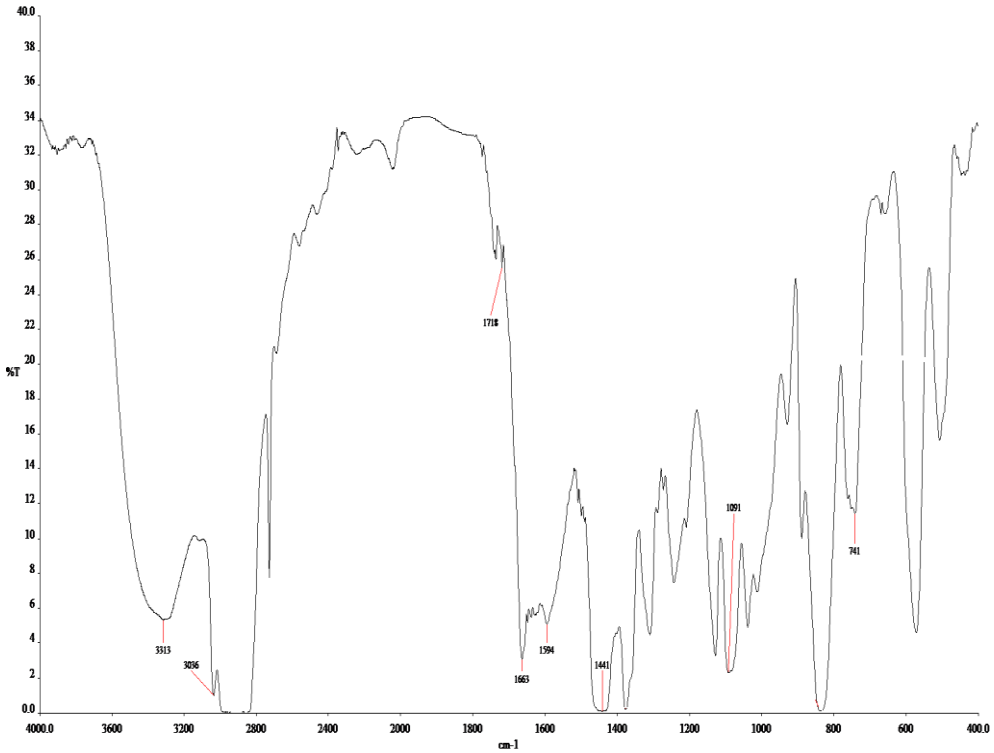

(h) NBR/1.5 wt% GO Cured for 3 Hours

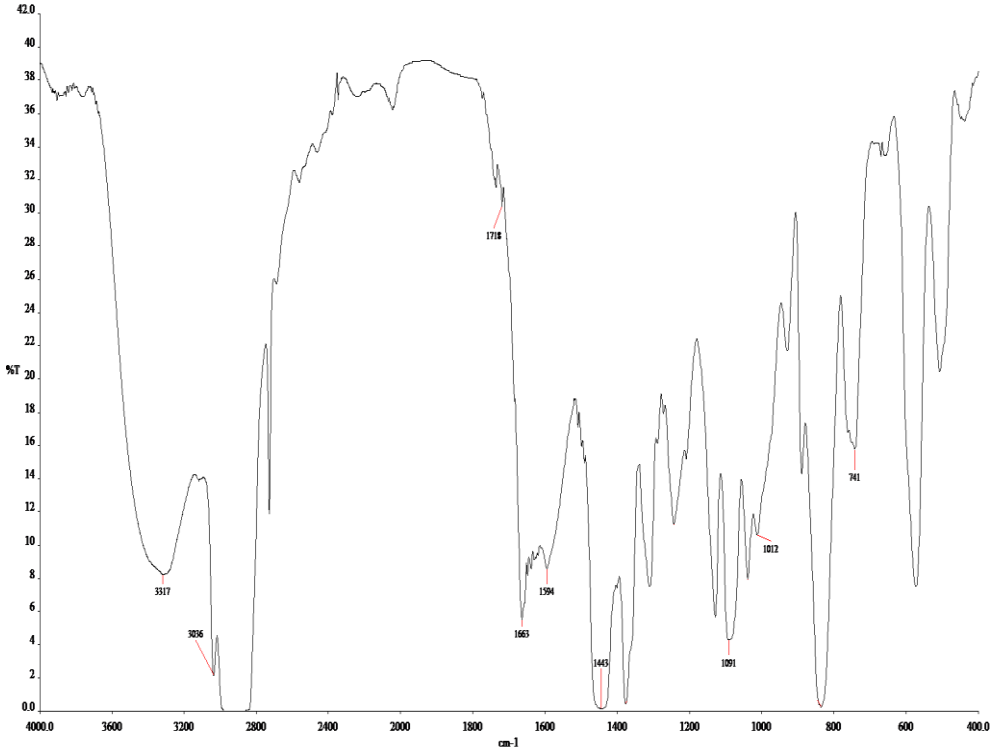

(i) NBR/2.0 wt% GO Cured for 2 Hours

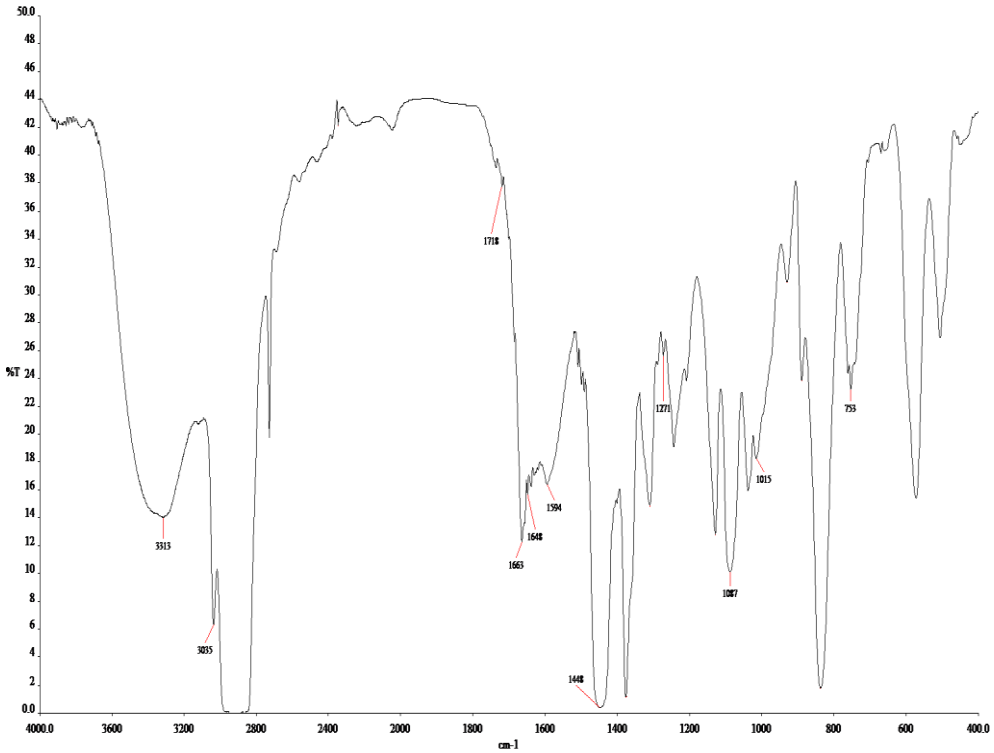

(j) NBR/2.0 wt% GO Cured for 3 Hours

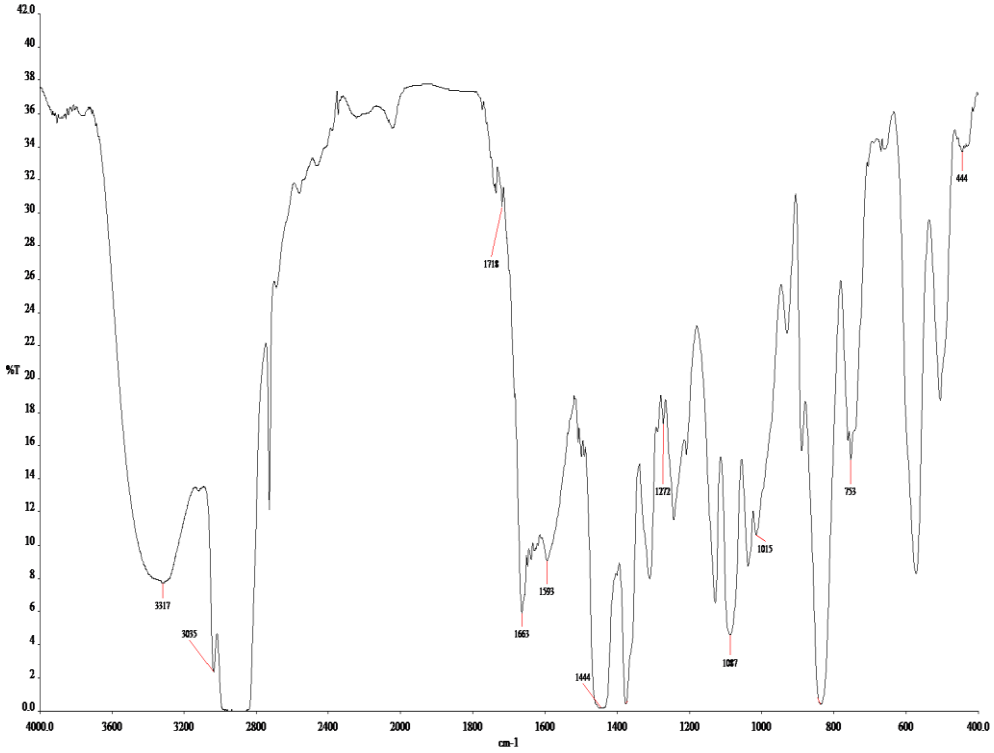

APPENDIX B: Field Emission Scanning Electron Microscopy (FESEM)

(a) NBR Cured for 2 Hours at (i) X500 and (ii) X1000

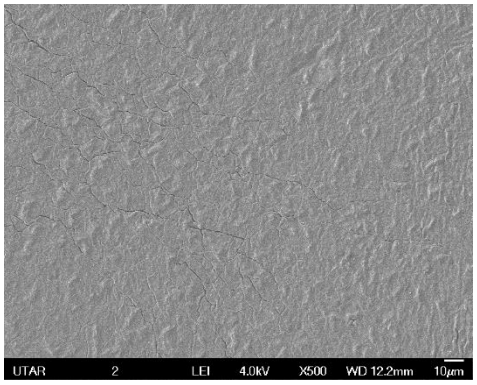

(i)

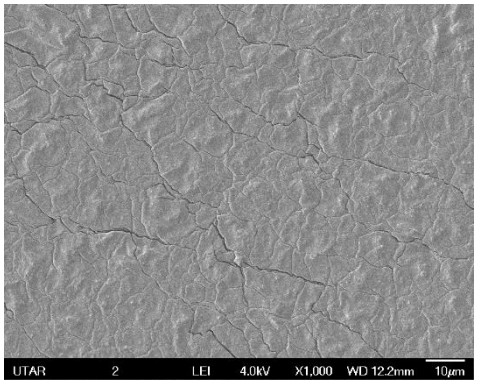

(ii)

(b) NBR Cured for 3 Hours at (i) X500 and (ii) X1000

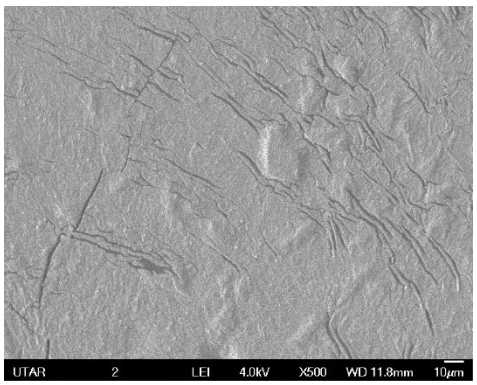

(i)

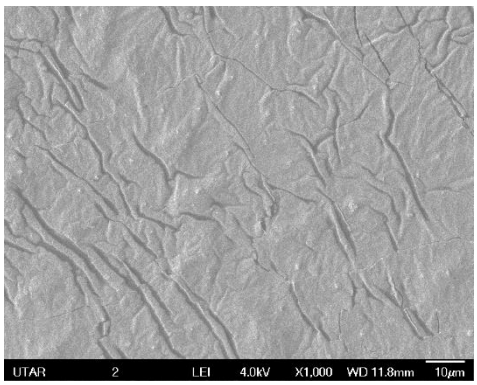

(ii)

(c) NBR/0.5 wt% GO Cured for 2 Hours at (i) X500 and (ii) X1000

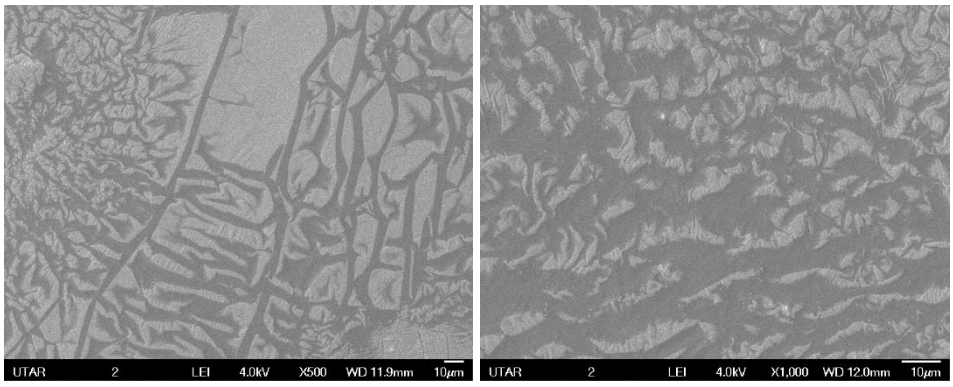

(i) (ii)

(d) NBR/0.5 wt% GO Cured for 3 Hours at (i) X500 and (ii) X1000

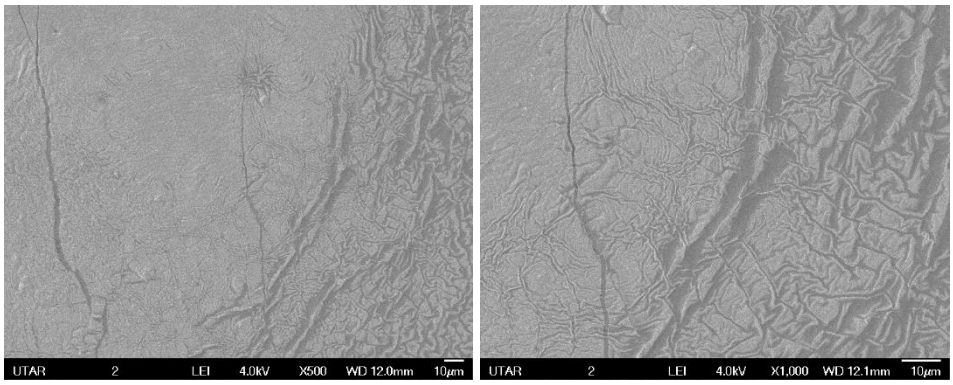

(i) (ii)

(e) NBR/2.0 wt% GO Cured for 2 Hours at (i) X500 and (ii) X1000

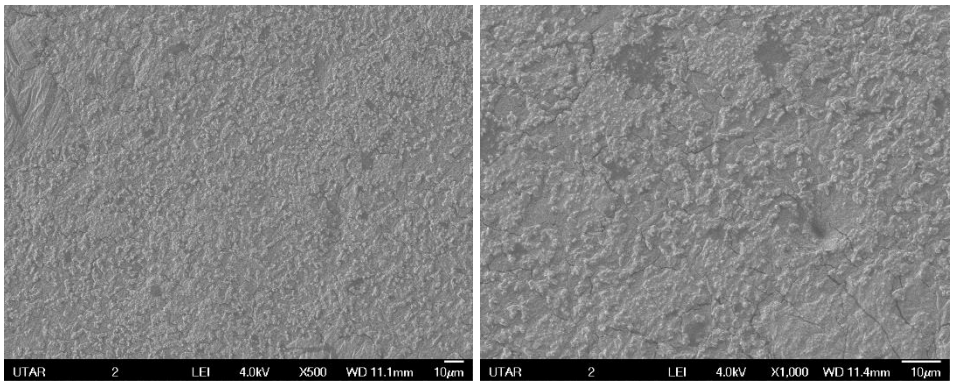

(i) (ii)

(f) NBR/2.0 wt% GO Cured for 3 Hours at (i) X500 and (ii) X1000

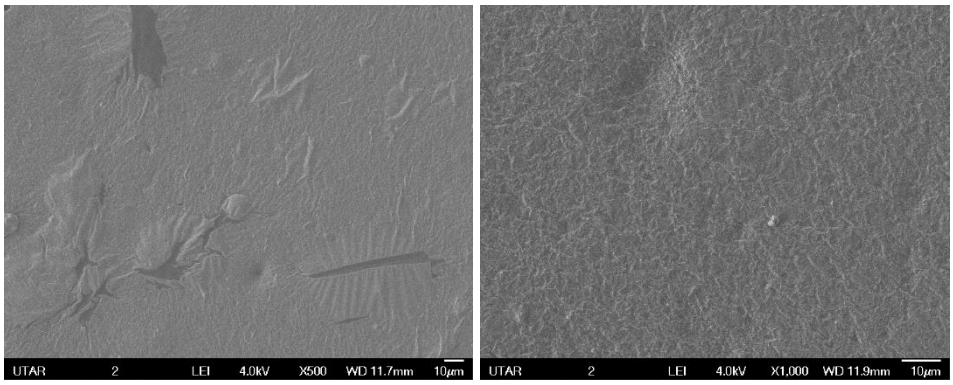

(i) (ii)